https://doi.org/10.32604/zkg.2026.074665

REVIEW

Advances in steel slag modification and synergistic mechanisms via multi-source solid waste integration for performance enhancement

Jianshuai Hao[1], Kuizhen Fang[1], Zihan Zhou[1,2,*] and Shiyu Zhuang[1,3,*]
[1]Department of Civil Engineering, Tsinghua University, Beijing, 100084, China
[2]College of Geological Engineering and Geomatics, Chang'an University, Xi'an, 710064, China
[3]Department of Civil and Environmental Engineering, The Hong Kong Polytechnic University, Hong Kong, 999077, China
*Corresponding Authors: Zihan Zhou. Email: zhouzh@chd.edu.cn; Shiyu Zhuang. Email: mini_zhuang@163.com

Received: 15 October 2025; Accepted: 25 December 2025

ABSTRACT: Steel slag (SS), a major solid by-product of the steel industry, holds significant potential for use in construction materials due to its high calcium content and latent pozzolanic activity. However, its large-scale utilization is limited by challenges such as low reactivity and poor volumetric stability. This paper provides a comprehensive review of the physicochemical properties and cementitious mechanisms of basic oxygen furnace slag (BOFS), electric arc furnace slag (EAFS), and ladle furnace slag (LFS). It critically evaluates the effectiveness and limitations of five modification strategies—mechanical activation, chemical treatment, thermal processing, carbonation, and *in-situ* modification—in enhancing SS reactivity and stability. Furthermore, it explores the synergistic mechanisms and current research on the combined use of SS with high-calcium, high-alkalinity, high-sulfate, and silica-alumina-rich solid wastes (e.g., granulated blast furnace slag, fly ash, silica fume, and red mud), and summarizes the latest advancements in multi-component, low-carbon cementitious systems. In addition, the potential applications of SS in non-construction fields, such as mine backfilling and expansive soil stabilization, are discussed, providing theoretical foundations and technical pathways for its high-value utilization and contribution to carbon neutrality goals.

KEYWORDS: Steel slag; activation mechanisms; multi-source solid waste integration; synergistic mechanisms; performance enhancement

MATERIALS

1 Introduction

The steel industry, a fundamental pillar of the global economy, is a major generator of industrial solid waste and ranks among the largest contributors to solid-waste emissions. The production of one tonne of crude steel requires approximately 0.96 t of pig iron and yields 0.2–0.4 t of SS, 80–100 kg of sinter flue-gas desulfurization ash (FDA), and 0.7–1.2 t of granulated blast furnace slag (GBFS) [1–3]. As illustrated in Figure 1, global crude steel output reached 1.8785 billion t in 2022, implying that SS generation exceeded 225 million t globally [4, 5]. China, accounting for 56.7% of global steel production, generated over 1 billion tonnes of SS between 2011 and 2022. However, its comprehensive utilization rate remains below 30%—significantly lower than that of Europe, the United States, and Japan [6–10]. The underutilization of SS not only consumes valuable land resources but also presents long-term environmental risks, given its high alkalinity and the potential for heavy metal leaching into soil and groundwater through rainfall infiltration [11, 12]. Concurrently, ordinary Portland cement (OPC) production remains highly carbon-intensive, emitting approximately 0.8 t of CO_2 per tonne of cement, with the extensive global consumption of cement, the building materials industry consequently accounts for about 8% of global carbon emissions [13, 14]. In this context, the efficient valorization of SS, GBFS, and associated industrial by-products into low-carbon cementitious materials emerges as a critical strategy for improving resource efficiency and advancing carbon neutrality objectives.

Among the numerous by-products of the steel industry, SS is particularly noteworthy due to its large output, low utilization rate, and high environmental risks. SS is rich in highly crystalline silicate minerals that exhibit inherently slow hydration kinetics. As a result, its use as a direct replacement for cement often leads to suboptimal mechanical properties and insufficient durability for engineering applications. Furthermore, SS

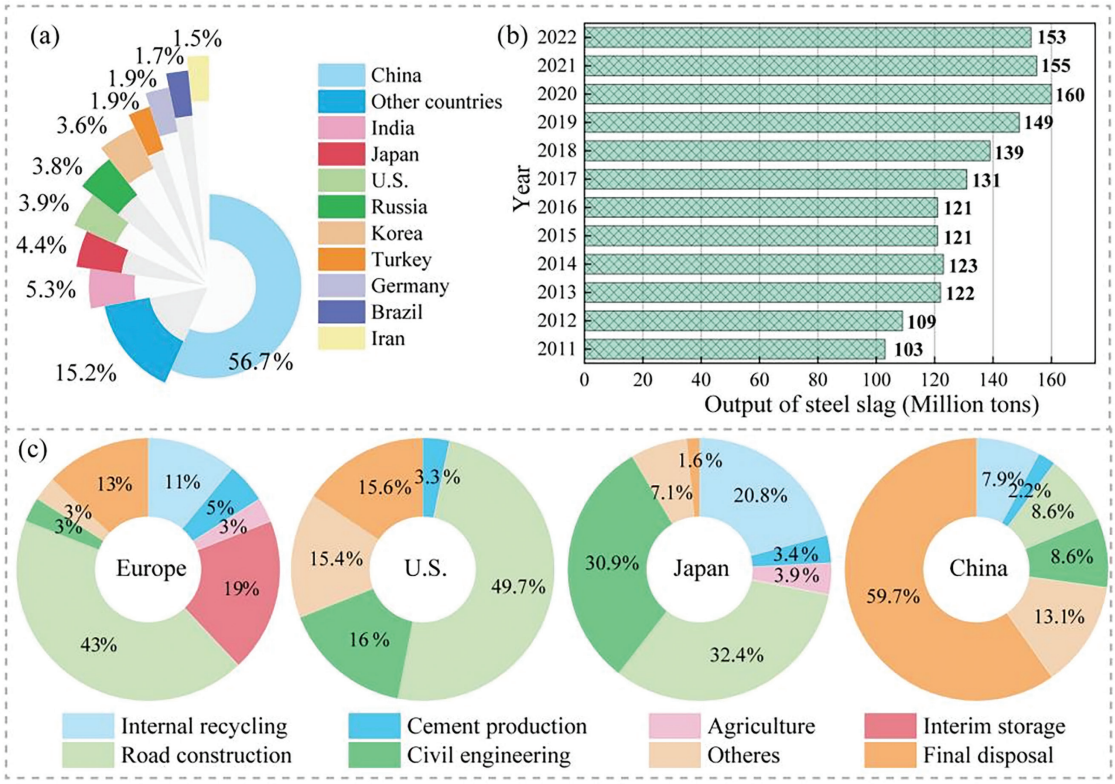

1 Landscape of crude steel production and SS utilization [4, 5]. (a) Global crude steel production and geographic distribution; (b) Annual SS generation in China, 2011–2022; (c) Comprehensive utilization rates of SS across countries

often contains f-CaO and f-MgO. Under humid or cyclic wet-dry conditions, these compounds can undergo delayed hydration, leading to destructive expansion and cracking, this volume instability poses a major technical barrier to its use as a cement substitute at high replacement ratios. To enhance its reactivity and maintain performance at high substitution levels, current strategies focus on mechanical activation, chemical activation, and thermal treatment [15–18]. However, these methods are often energy-intensive and economically burdensome, limiting their scalability. In contrast, composite utilization strategies that exploit synergistic interactions among industrial by-products—such as GBFS, fly ash (FA), and phosphogypsum (PDG)—have demonstrated the potential to overcome the intrinsic limitations of standalone SS systems [19–22]. For instance, reactive aluminum-bearing phases in GBFS facilitate the depolymerization of SS's silicate network [23, 24], while sulfate ions from PDG accelerate AFt formation, jointly enhancing early-age strength development [25, 26]. This "waste-for-waste" approach enables large-scale consumption of industrial residues, reduces carbon emissions and energy input during binder production, and promotes a circular model of resource utilization. Nevertheless, despite recent advancements, the interactions within multicomponent solid-waste binder systems remain poorly understood. The hydration and hardening mechanisms, as well as the physicochemical basis of inter-residue synergies, require comprehensive synthesis and further investigation.

Against this backdrop, this review consolidates current knowledge on the physicochemical properties, cementitious components, and microstructural characteristics of various types of SS. It systematically presents methods and recent advancements aimed at enhancing cementitious reactivity and volumetric stability, and analyzes the performance and interactive mechanisms of blended binders incorporating SS with GBFS, FA, silica fume (SF), and red mud (RM). Furthermore, the review evaluates emerging applications beyond conventional construction, particularly in mine backfilling and the stabilization of expansive soils. Overall, it seeks to promote the transition from passive stockpiling to efficient resource utilization, mitigate environmental impacts, and provide both theoretical foundations and practical guidance for the development of high-performance, low-carbon binder systems based on SS.

2 Fundamental characteristics of steel slag

2.1 Formation and classification

Steelmaking is fundamentally an oxidation and refining process, wherein fluxes such as lime, dolomite, fluorite, and silica are introduced to

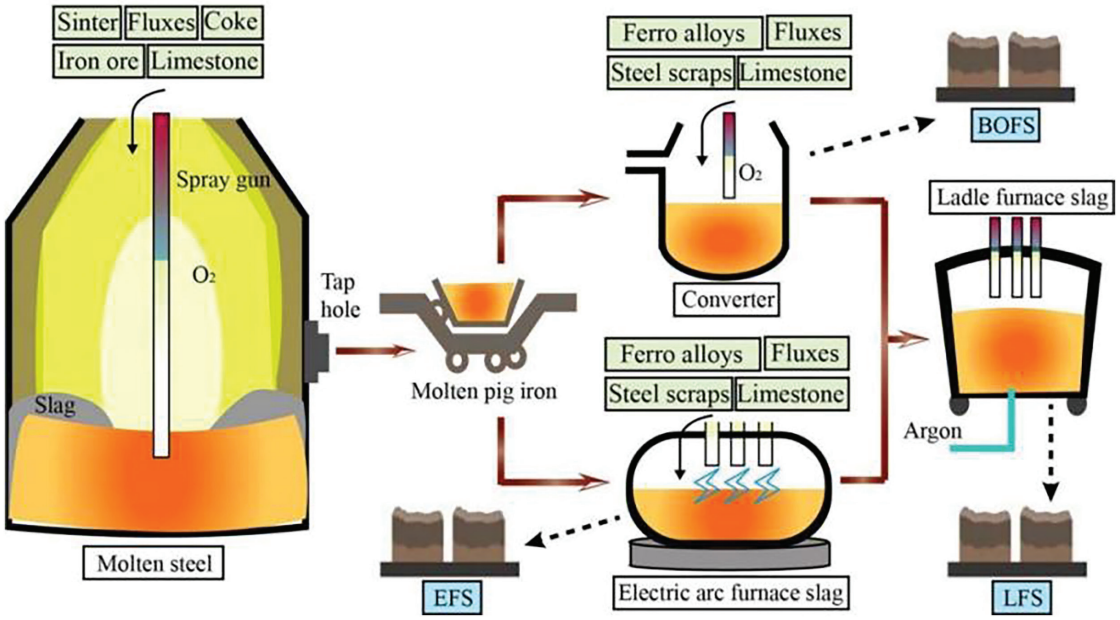

2 Generation routes and classification of SS

remove impurities (e.g., Si, Mn, P, S) from hot metal, resulting in an iron–carbon alloy with a controlled composition. Based on the production route, SS is typically classified into three main types (Figure 2): BOFS, EAFS, and LFS. BOFS is produced during primary refining in the blast furnace–basic oxygen furnace (BF–BOF) route, where hot metal and scrap undergo intense carbon–oxygen reactions. This process results in rapid slag–metal separation and yields a high slag volume, comprising approximately 70–75% of total SS output [27–29]. EAFS originates from the electric arc furnace (EAF) route, in which scrap steel is melted via arc heating and impurities are transferred to the slag phase. EAFS accounts for roughly 28.6% of global SS production according to multiple datasets [27, 30]. Owing to high operating temperatures and flexible process control, the EAF route supports efficient scrap recycling. EAFS is typically enriched in FeO, MgO, and RO (divalent metal oxide) solid solutions, and is distinguished by high density and favorable volumetric stability. LFS is generated during the secondary steelmaking stage, specifically in the ladle furnace (LF) refining process that follows primary refining via either the BOF or EAF route. This post-refining step is critical for attaining the desired chemical composition of molten steel. Key functions of LF refining include final desulfurization, removal of non-metallic inclusions, and, when necessary, final decarburization. The resulting slag is typically rich in Cr_2O_3, C_2S, and spinel phases. Rapid carbonation and possible heavy-metal leaching require strict environmental controls to limit ecological risk. To highlight the commonality of modification methods, the term "SS" will be used as a general designation in the subsequent text.

2.2 Physicochemical properties

The formation history, chemical composition, and physical properties of each SS type are tightly coupled to its parent metallurgical process, which in turn determines distinct valorization pathways (Tables 1 and 2). BOFS typically contains high levels of CaO (40–55%) and total Fe (13.6–29.5%), with a basicity ratio (CaO/SiO_2) ranging from 2.3 to 3.5. Its hard and brittle structure leads to poor grindability (Mohs hardness 6–8), necessitating the use of grinding aids such as gypsum, calcium chloride, or ethanol. BOFS is commonly utilized as a clinker substitute, road base material, sinter return, and precursor for alkali-activated binders. Due to its elevated contents of f-CaO and f-MgO [30–33], pre-aging is typically required to enhance dimensional stability. Relative to BOFS, EAFS contains less CaO (25–35%) but more total Fe (22–35%) and SiO_2 (12–20%), yielding a lower basicity. It is enriched in FeO, MgO, and RO (divalent metal oxide) solid solutions. EAFS exhibits high density and hardness (Mohs 6–7), along with good volumetric stability [33–38]. Its grindability can be improved through granulation, rapid quenching, or co-grinding with softer materials. These enhancements expand its applications to asphalt aggregates, blasting abrasives, carbon-cured products, and alkali-activated gel systems. LFS is characterized by high contents of Al_2O_3 (25–30%) and CaO (>50%), along with superior intrinsic reactivity, high grindability, and the most favorable volumetric stability among the three slag types [33]. As a high-alumina supplementary material, LFS is particularly suitable for

Table 1 **Chemical composition of SS from the researched literature (wt%)**

SS	Ref.	CaO	Fe Total	SiO_2	Al_2O_3	MgO	MnO	SO_3	P_2O_5	$Na_2O + K_2O$
BOFS	[30]	55.20	24.84	9.92	2.14	1.52	2.15	0.64	1.46	1.52
	[31]	40.80–49.80	13.60–22.40	13.6–15.2	4.0–5.1	5.1–7.4	2.2–3.2	–	–	–
	[32]	40.82–54.29	16.78–29.49	8.45–16.93	0.33–5.85	1.93–9.15	1.2–8.7	0.07–0.71	0.89–7.14	0.27–0.84
	[33]	41.03	27.03	16.15	4.31	3.64	–	0.16	–	0.37
EAFS	[30]	33.56	29.47	16.26	8.05	4.88	4.58	0.12	0.59	–
	[38]	24.73	34.50	19.89	–	4.058	4.936	0.532	0.436	–
	[32]	25.08–45.90	22.30–38.51	12.2–20.3	1.55–12.2	2.82–7.68	1.3–5.87	0.42–0.65	0.5–1.37	0.62–0.63
LFS	[35]	51.67	–	29.62	3.63	6.66	0.42	0.498	0.466	0.06
	[36]	58.90	0.30	25.2	7.7	4.4	–	1.9	–	–

Table 2 **Physical properties and mineral composition of different SS [37–41]**

SS Type	BOFS	EAFS	LFS
Density	3.2–3.5 g/cm³	3.3–3.7 g/cm³	3.0–3.2 g/cm³
Mohs hardness	6–8	6–7	5–6
Ease of grinding	Difficult to grind; high hardness and brittleness; strong sintering structure.	RO solid solution results in a dense, hard material, requiring multi-stage crushing	Easily ground; high glass content, low density
Volumetric stability	High f-CaO/MgO content, requires aging	Low f-CaO and f-MgO content	Low f-CaO, rapid cooling
Environmentally Sensitive elements	Minimal heavy metals	Cr, V	High Al content, aids desulfurization
Main applications	Road base, clinker replacement, metallurgical recovery	Alkali-activated cementitious materials, sandblasting abrasives	Self-leveling mortars, carbon-cured binders

self-leveling mortars, autoclaved aerated concrete, and rapid-setting repair formulations in sustainable construction systems.

2.3 Reactive constituents and microstructure of steel slag

While SS exhibits certain similarities to OPC clinker in its major chemical composition (e.g., being rich in calcium and silicon) (Figure 3) [42]. The principal crystalline phases include C_3S, C_2S, dicalcium ferrite (C_2F), calcium aluminate ($C_{12}A_7$), and an RO phase (a solid solution of divalent metal oxides such as CaO, FeO, MgO, and MnO) (Figure 4a–c). Accessory phases may comprise calcite ($CaCO_3$), magnesioferrite ($MgFe_2O_4$), calcium ferrite–aluminate ($CaAl_8Fe_4O_{19}$), ferrous/magnesian silicates ($(Mg,Fe)_2SiO_4$), free lime and periclase (f-CaO, f-MgO), and wüstite (FeO) [43, 44]. Pang et al. [45] and Wang et al. [46] reported that the main hydration products of SS pastes are C–S–H gel and CH. However, due to inherently slow reaction kinetics, hydration progresses over prolonged periods and results in limited product formation; after 360 d, the chemically bound water content in hydrated SS remains only slightly above 60% of that observed in OPC. The low reactivity of BOFS is primarily attributed to its high iron oxide content, extensive polymorphic transformations, and microcrystalline structure formed under elevated melt temperatures and slow cooling rates [47–49]. Compared with BOFS, EAFS generally contains more iron and less calcium, and its predominantly

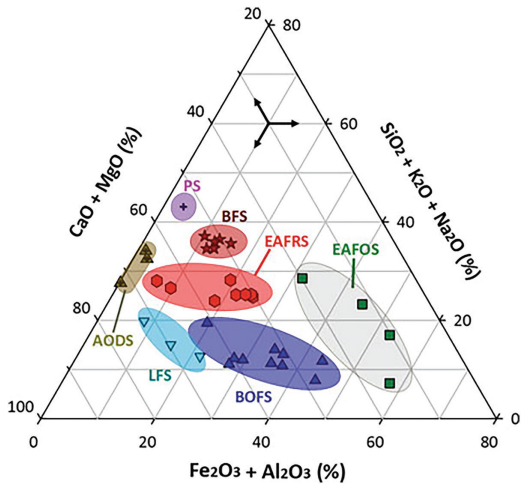

3 **Normalized CaO(MgO)–SiO_2(Na_2O, K_2O)–Al_2O_3(Fe_2O_3) phase diagram for various types of SS [42]**

crystalline microstructure further reduces reactivity [50, 51]. In LFS, C_2S is abundant and exists in multiple polymorphs, undergoing sequential transformations during cooling. When air-cooled at moderate rates to approximately 675°C, α-C_2S converts to β-C_2S; further cooling to 400–500°C leads to the formation of γ-C_2S. Due to density differences among these polymorphs, the β → γ transformation induces a volumetric expansion of approximately 10–12%, causing disintegration (or "dusting") of the SS into fine particulates. The

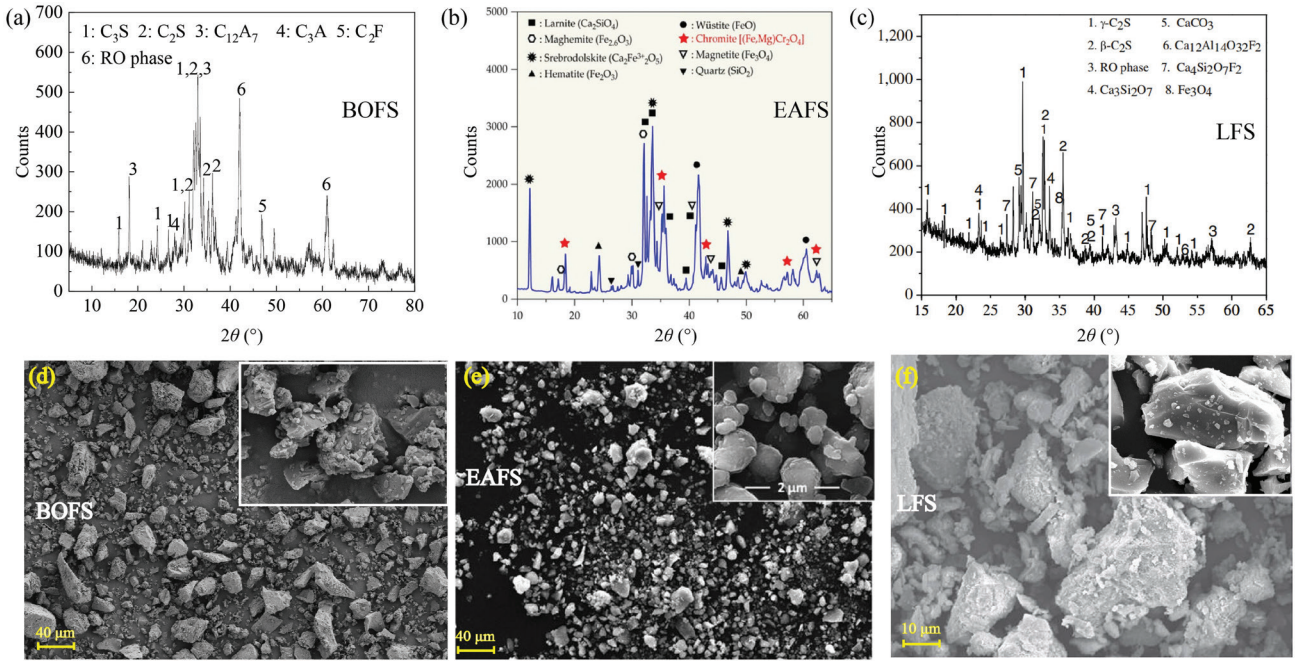

4 (a) XRD pattern of BOFS [42]; (b) XRD pattern of EAFS [43]; (c) XRD pattern of LFS [44]; (d) SEM images of BOFS [42]; (e) SEM images of EAFS [54, 55]; (f) SEM images of LFS [56, 57]

γ-C_2S polymorph remains stable below 850°C, exacerbating this issue [52, 53].

Scanning electron micrographs (SEM) presented in Figure 4d–f illustrate the morphological characteristics of SS particles [42, 54–57]. BOFS and EAFS exhibit subrounded to angular shapes with rough surfaces bearing fine, irregular adherent particles—features likely resulting from thermodynamic disequilibrium during solidification [58, 59]. Specifically, BOFS particles predominantly exhibit an irregular, angular morphology, often with abundant honeycombed or irregular pore structures adhering to their surfaces. In contrast, EAFS particles tend to be sub-rounded in shape and frequently display plate-like crystalline structures. Furthermore, the surface morphology of EAFS is generally rougher and more complex, characterized by distinct grain boundaries, a more developed porous network, and the presence of larger, unevenly distributed pores. LFS particles, by comparison, have smoother surfaces, more uniform particle-size distribution, indistinct grain boundaries, and smaller, more evenly distributed pores.

3 Strategies to enhance the reactivity and volumetric stability of steel slag

The low intrinsic reactivity of SS, coupled with concerns over volumetric stability, remains a primary obstacle to its large-scale utilization. To address these limitations, five principal activation strategies have been developed: mechanical activation, chemical activation, thermal activation, carbonation activation, and *in-situ* modification activation.

As shown in Table 3, these methods differ significantly in their processing mechanisms, implementation complexity, and overall benefits. Mechanical activation, which relies mainly on physical grinding, offers notable advantages such as a simple process, low energy consumption, low processing costs, high technological maturity, and good environmental compatibility. However, its ability to activate inert mineral phases—such as the RO phase and crystalline C_2S/C_3S—remains limited. Chemical activation, involving the introduction of alkaline, acidic, or salt-based reagents, can effectively enhance early-age hydration activity and accelerate heat release. Nonetheless, it faces challenges including reagent dependency and wastewater treatment, and its applicability is influenced by the chemical composition of the SS. Thermal activation, employing high-temperature or hydrothermal conditions, significantly improves reactivity and early-age mechanical properties, making it particularly suitable for producing high-performance materials. However, this approach requires substantial equipment and energy inputs. Carbonation activation enhances reactivity while enabling CO_2 sequestration, representing a promising low-carbon technology. Among carbonation routes, the indirect extraction–re-carbonation process demonstrates relatively high efficiency, whereas direct gas–solid carbonation suffers from harsh reaction conditions and low efficiency; the overall process also remains dependent on a CO_2 source or chemical extractants. *In-situ* modification involves melt regulation or stoichiometric design to fundamentally reconstitute the mineral composition of SS, thereby improving both reactivity and long-term

Table 3 **Comparative analysis of SS modification methods**

Method	Mechanical Activation	Chemical Activation	Thermal Activation	Carbonation Activation	*In-Situ* Modification
Process complexity	Relatively simple; primarily physical processes.	Moderately complex; requires an activator.	More complex; requires high-temperature treatment.	Moderately complex; requires a CO_2 environment.	More complex; requires precise process control.
Cost	Low	Medium	Medium	Medium	High
Resource consumption	Primarily consumes electricity and grinding media.	Consumes chemical activators.	Energy-intensive; requires heating equipment.	Requires large amounts of CO_2	Energy-intensive; requires precise process control.
Environmental impact	Negligible impact	Requires recovery of chemical reagents	Due to high energy consumption	Carbon sequestration effect	High-temperature processing
Applicability	Applicable to most SS types.	Requires tailoring the activator to the SS type	Suitable for materials with high performance requirements	Suitable for low-carbon building materials	Suitable for high-value-added applications
Solid waste valorization efficiency	Moderate	High	High	via carbon capture and utilization	High
Technology maturity	Mature	Fairly mature	Fairly mature	Pilot stage	Research & development

volume stability. However, this approach currently entails the most complex process design, the highest energy and capital investment costs, and most solutions remain at the laboratory research or pilot stage, with considerable progress still needed for large-scale industrial application.

3.1 Mechanical activation

Mechanical activation through grinding markedly increases the fineness of SS and thereby enhances its hydration reactivity. Under high-energy mechanical forces (impact, shear, friction), robust bonds such as Si–O and Ca–O are cleaved, and portions of the crystalline matrix transform into amorphous or metastable structures with a higher density of reactive sites [60–63]. Numerous studies have demonstrated a positive correlation between fineness and reactivity [64, 65]. Duan et al. [66] used a supersonic steam jet mill (model S-FW 200) to perform ultrafine grinding of SS. This treatment increased the specific surface area from 475 m^2/kg to 768 m^2/kg and raised the 28-day activity index from 45% to 80%. In a study by Shi et al. [67], SS was initially subjected to multiple comminution stages—including a jaw crusher, roller crusher, and ball mill—to obtain raw materials of different size classes, followed by ultrafine grinding in a superheated steam jet mill. The results showed that as the median particle size (D_{50}) of the SS powder decreased to 13.3, 8.11, 5.10, and 2.52 µm, the corresponding activity indices increased to 78%, 82%, 87%, and 95%, respectively. In another work, Santos et al. [68] employed a Retsch RS 300 XL disc mill to reduce the particle size of SS from 56 µm to 16 µm. While Liu and Li [69] increased specific surface area from 3890 to 6350 cm^2/g; in both cases, cumulative heat release within 90 h more than doubled. This pronounced sensitivity is largely attributed to the particle-size-dependent reactivity of C_2S, which is the dominant phase in BOFS [70–72]. For SS with poor grindability or a strong tendency to agglomerate, particularly BOFS, wet grinding or the addition of grinding aids such as glycerol, triethanolamine, and calcium lignosulfonate at approximately 0.05 weight percent of SS can significantly improve milling efficiency [73, 74]. Polar organic additives containing hydroxyl or hydroxylamine groups are especially effective [75, 76]. By forming a stable adsorbed film on particle surfaces, they reduce interfacial energy, suppress agglomeration, neutralize unsaturated surface charges, and promote crack propagation (Figure 5). Although the mechanical activation

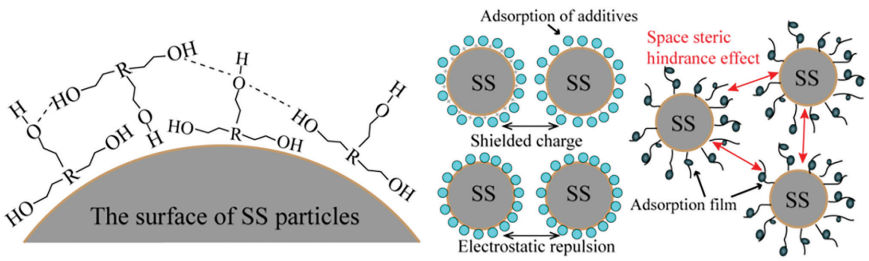

5 **Schematic illustration of the adsorption and dispersion of grinding aids on the surface of SS particles [75, 76]**

method involves significant energy consumption and costs during the grinding process, it still offers a relative cost advantage compared to other activation methods. However, the attainable increase in reactivity is limited, so in practice it is often combined with other activation strategies.

3.2 Chemical activation

Chemical activation involves the use of added reagents to modify the mineralogical assemblage of SS, thereby significantly enhancing its cementitious reactivity. The principal categories of chemical activators include alkalis, acids, and salts. Among these, alkaline activation is the most widely employed, with hydration behavior primarily influenced by the type and concentration of the activator. Common alkaline agents include sodium- and potassium-based compounds such as silicates, hydroxides, sulfates, and carbonates [77–82]. By increasing the number of nucleation sites and raising pore-solution alkalinity, alkaline activation promotes the depolymerization and hydration of key reactive phases such as C_3S and C_2S. Although nominally inert components exhibit limited activity, SS systems as a whole often show substantial reactivity under strong alkaline conditions, yielding C-(A)-S-H gels and crystalline CH as the main hydration products [83–87]. Elevated initial alkalinity not only accelerates early hydration but also enhances volumetric stability; even RO solid solutions have demonstrated measurable activity in highly alkaline environments [88, 89].

Acid activation represents an effective complementary approach, particularly in overcoming the limitations associated with alkali-activated SS systems. Strong mineral acids (e.g., H_2SO_4, HCl) promote the dissolution of calcium-, iron-, and aluminum-rich phases, disrupt passivating surface layers, and enhance the mobility and polymerization of silicoaluminate species. Notably, organic acids such as acetic, phosphoric, and oxalic acid often exhibit superior leaching efficiency compared to their inorganic counterparts [90–93]. For instance, acetic acid dissolves $Mg_2Al(OH)_7$, f-CaO, C_3S, C_2S, C_2F, and RO phases, thereby releasing Ca^{2+} and promoting subsequent hydration; as its concentration increases, product particle size tends to grow while total porosity decreases [94]. Oxalic acid, on the other hand, precipitates Ca^{2+} as calcium oxalate (CaC_2O_4), thereby reducing calcium saturation and improving the reactivity of remaining phases [95].

In summary, chemical activation can substantially improve both the reactivity and mechanical performance of SS-based binders. However, the optimal selection of activator is highly dependent on SS type, which limits general applicability. In addition, chemical activation may increase energy consumption and introduce environmental burdens associated with the recovery and treatment of chemical solutions. Future research should therefore focus on developing low-energy, environmentally benign activators to support the sustainable implementation of chemically activated SS systems.

3.3 Thermal activation

Thermal activation enhances the hydration reactivity of SS by providing sufficient thermal energy to cleave strong chemical bonds (e.g., Si–O and Al–O), depolymerize the glassy matrix, and increase the density of reactive sites [96, 97]. At high temperatures (600–1000°C), CaO preferentially reacts with dissolved silica to form C–S–H, whereas MgO interacts with residual silica to generate M–S–H phases [98]. Two primary thermal activation strategies have been employed [99, 100]: (i) external heating, typically achieved through autoclave or steam curing (400–800°C), and (ii) internal thermal activation, which utilizes the exothermic heat released during binder hydration and other reactions when SS is incorporated into cementitious matrices (hydrothermal/steam activation at approximately 100–250°C). Thermally treated SS powders generally exhibit accelerated hydration kinetics and improved early-age mechanical performance [101, 102]. As the activation temperature increases (65°C), the main exothermic peak shifts to earlier time points, the cumulative heat release rises, and the setting time is notably reduced [103]. Overall, thermal activation represents a promising route for developing high-performance SS-based binders. Nevertheless, its relatively high energy demand necessitates a balanced assessment of performance gains versus energy input. To enhance sustainability in practical applications, future research should focus on improving energy efficiency by adopting lower-temperature activation techniques and integrating renewable or low-carbon thermal energy sources.

3.4 Carbonation activation

Accelerated carbonation of SS represents a promising pathway for developing low-carbon construction materials. This approach not only enhances the performance of SS-containing products but also enables simultaneous CO_2 sequestration, thereby promoting large-scale recycling and resource circularity [104, 105]. As illustrated in Figure 6, reactive components such as f-CaO, f-MgO, C_3S, and the polymorphs of dicalcium silicate (β-C_2S and γ-C_2S) undergo carbonation in CO_2-rich environments (Figure 6a) [106, 107]. Concurrently, leached Ca^{2+} precipitate with CO_3^{2-} derived from dissolved CO_2, leading to the formation of a porous carbonate layer on the SS particle surfaces (Figure 6b) [108]. When carbonated SS is utilized as a supplementary cementitious material in OPC systems (Figure 6c), the modified particle surfaces act as additional nucleation sites for C–S–H, thereby accelerating early C–S–H formation and improving early-age strength development in carbonated SS-based cementitious materials (CS-CM) [109, 110]. In addition to the nucleation effect, carbonated SS also participates synergistically in hydration reactions

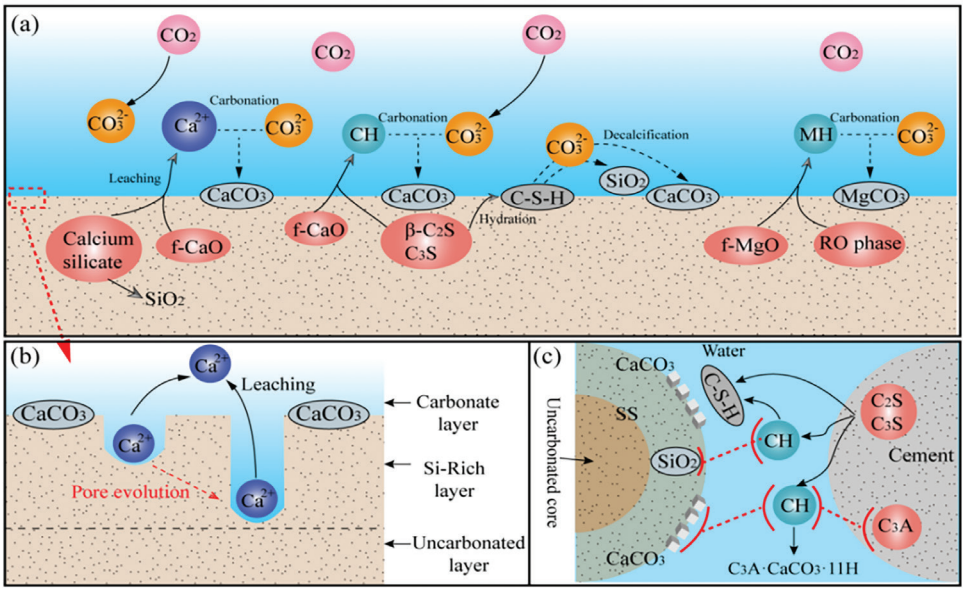

6 (a) Carbonation process and mechanism of SS [106, 107]; (b) Surface morphology of SS particles after carbonation [108]; (c) Synergistic mechanism between carbonated SS and cement [109, 110]

with OPC. The formation of amorphous SiO_2 and finely dispersed $CaCO_3$ within the slag is considered a key factor contributing to the enhanced reactivity of CS-CM composites [111].

Carbonation can proceed via two main pathways: direct and indirect routes [112]. Direct carbonation involves reacting the slag with CO_2 without the use of chemical extractants, typically under elevated temperature and CO_2 pressure in dry, humid, or aqueous environments. In this one-step process, calcium leaching and carbonate precipitation occur simultaneously, although the overall carbonation efficiency tends to be limited [113–115]. For instance, BOFS carbonated at 650°C under 20 bar CO_2 pressure achieved only 9–26% conversion [116], while gas–solid carbonation at 500°C for 50 min yielded maximum conversions of 18% for BOFS and 29% for EAFS [117]. In contrast, indirect carbonation—which relies on prior extraction of Ca^{2+} and Mg^{2+}—can achieve significantly higher conversion rates, often approaching 90%, even under ambient temperature and pressure conditions [118–120]. To enhance leaching efficiency, various extractants have been employed, including inorganic acids (HCl, HNO_3, H_2SO_4), organic acids (e.g., acetic acid), and ammonium-based salts (NH_4Cl, NH_4NO_3, $(NH_4)_2SO_4$, NH_4HCO_3) [121, 122]. Additionally, process parameters such as reduced particle size, elevated reaction temperatures, lower solid-to-liquid ratios, and the application of ultrasonic agitation have been demonstrated to further improve leaching and carbonation kinetics [123, 124]. Carbonated SS powders exhibit increased pozzolanic activity, promote clinker hydration, elevate the total heat release during cement hydration, shorten setting times, and enhance the mechanical performance of mortars [125, 126]. Overall, carbonation activation offers substantial sustainability benefits and serves as a viable strategy for the development of low-carbon building materials, with strong potential for integration into carbon capture and resource recovery frameworks.

3.5 In-situ modification

In-situ modification is an efficient technique that involves molten-state regulation of SS during its high-temperature liquid phase by introducing component-adjusting materials rich in Ca, Si, and Al (e.g., GBFS, FA, iron tailings) to regulate melt chemistry and viscosity [127, 128]. By precisely tuning the stoichiometric ratios and rheology of the melt, crystallization pathways can be steered during cooling, rebuilding the phase assemblage and markedly promoting the formation of highly reactive minerals such as C_3S and C_2S. Inert or weakly reactive phases (e.g., periclase and the RO solid solution) are transformed into reactive calcium silicates and aluminates (C_3S, C_2S, C_3A), accompanied by rupture and reorganization of Si–O and Al–O bonds that generate new reactive sites [129]. Concurrently, ferric oxides are converted to magnetite, MgO combines with Fe to form stable magnesioferrite, and expansive constituents such as f-CaO are suppressed, yielding comprehensive improvements in both cementitious reactivity and volumetric stability [130]. The choice of conditioning agent strongly modulates the reconstruction outcome. Lime increases the C_3S content and grain uniformity, refining the microstructure and enhancing mechanical performance [131]. FA can sequester f-CaO and stabilize the RO phase, while promoting the formation of silicates such as melilite and pyroxene, thereby improving durability [132]. Perlite refines crystal size, increases the glassy fraction, and raises hydration reactivity [133]. In a related approach, He et al. [134] used bituminous coal as a reductant to convert Fe_2O_3 with a 95% reduction rate, boosting the activity indices of the resultant residue to 114% at 7 d and 117% at 28 d,

which significantly enhanced cementitious performance. Although in-line reconstruction remains at the research and development stage, it addresses reactivity and soundness at the source and shows promising prospects for solid-waste valorization and green building materials.

4 Synergistic effects and mechanism analysis of SS-based cementitious systems

Steel slag is recognized as a promising cementitious precursor owing to its high calcium content. However, its relatively low silicon and aluminum contents constrain its performance when used as a standalone binder. The reactivity and mechanical properties of SS-based systems can be significantly improved by harnessing synergistic interactions with other industrial residues that effectively adjust the Ca/Si and Ca/Al ratios. Based on their predominant chemical compositions, these residues can be classified into four main categories (Figure 7): high-calcium, highly alkaline, sulfate-rich, and silica/alumina-rich materials.

High-calcium residues, such as GBFS, Class C fly ash (CFA) and carbide slag (CS)—are characterized by elevated CaO content. During hydration, they enhance the alkalinity of the pore solution and provide abundant calcium sources, thereby promoting extensive formation of C-S-H gels and contributing to both early-age and long-term strength development [135, 136]. Highly alkaline residues, including alkali residue (AR), coal gasification slag (CGS), and CS, are rich in Na_2O and K_2O. These constituents increase system pH, accelerate the dissolution of latent-reactive phases in SS, stimulate secondary hydration reactions, facilitate additional gel formation, refine pore structure, and enhance matrix densification and compactness [137, 138]. Sulfate-rich residues, such as desulfurization ash (DA), FDG, and

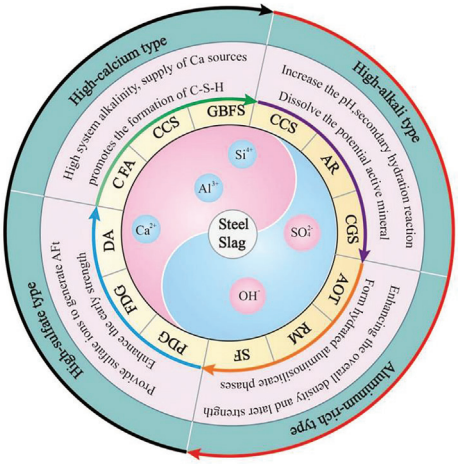

7 SS-based cementitious system incorporating multiple solid wastes

PDG—act as sulfate donors that promote the formation of abundant AFt. This not only contributes to early strength development but also improves dimensional stability, thereby mitigating the risk of shrinkage-induced cracking [139–141]. Silica/alumina-rich residues, including SF, RM, aluminous ore tailings (AOT), and certain high-alumina FA, contain high levels of reactive SiO_2 and/or Al_2O_3. Under alkaline conditions, these materials react synergistically with calcium- and sulfate-bearing components to form calcium aluminosilicate hydrates and related reaction products, resulting in matrix densification and enhanced later-age strength [142–144].

By integrating the complementary chemistries of these four material classes—and by strategically optimizing mixture proportions and interaction mechanisms—the latent reactivity of SS can be effectively activated, leading to significant enhancements in the performance of composite binder systems (Table 4). The following sections

Table 4 Case studies on the effects of different solid wastes on SS-based cementitious materials [145–149]

Ref.	Mechanism of Action	Mix Proportion	W/B	Performance
[145]	CS provides a rich source of Ca^{2+} and OH^- ions, which significantly accelerate the hydration process and promote the early formation of increased quantities of C-(A)-S-H gel and AFt.	CS:SS:GBFS:PG = 5:15:60:20	0.5	7 and 28 day strengths were 5 and 22 MPa, respectively.
[146]	LS actively consumes CH and facilitates the hydration of SS, leading to increased formation of C-(A)-S-H gel. Simultaneously, LS (lithium slag) contributes to pore structure refinement and a narrower pore-size distribution, resulting in a reduced most probable pore diameter.	OPC:SS:LS = 70:10:20	0.5	The measured flow spread was 201 mm. The UCS at 28 d reached 99.4% of the PC reference, while the 90-day UCS surpassed the reference, attaining 102.3% of PC.
[147]	The presence of SO_3^{2-} and OH^- in DA is crucial for facilitating the dissolution of C_2S and C_2F in SS.	DA:SS = 37.5:62.5	0.35	The initial flow spread was 185 mm; the 28- and 90-day strengths were 7.2 and 17.6 MPa, respectively.
[148]	EMR (electrolytic manganese slag) rich in $CaSO_4$, reacts with SS to produce copious needle-like AFt, which further accelerates hydration.	EMR:SS:GBFS = 50:20:30	0.4	The 28-day UCS reached 23.0 MPa, and the heavy-metal immobilization efficiency exceeded 90%.
[149]	MK (metakaolin) supplies reactive Al_2O_3 and SiO_2, consuming additional CH in the SS–cement system and yielding C-(A)-S-H with a lower Ca/Si ratio and a higher Al/Ca ratio.	OPC:SS:MK = 70:20:10	0.5	The initial flow spread was 173 mm, and the 28-day UCS was 53.13 MPa.

systematically explore the synergistic mechanisms and cementitious applications of four extensively studied industrial residues used in conjunction with SS: GBFS, FA, SF, and RM.

4.1 SS + GBFS based cementitious systems

The synergistic combination of SS with the chemically cognate industrial by-product GBFS for the development of clinker-free or low-clinker binder systems has emerged as a widely studied research direction. In binary SS+GBFS systems, increasing the SS content initially enhances UCS but subsequently leads to a decline beyond the optimal threshold [150, 151]. The best early- and late-age performance is typically observed at SS:GBFS mass ratios of 2:3 or 1:1, with reported 7-day and 28-day UCS of 16.5 and 31 MPa, respectively [152]. To further enhance hydration kinetics and early mechanical performance in clinker-free systems, additions of FDG or small dosages of OPC have proven effective in accelerating hydration and promoting rapid setting and hardening [153, 154]. In the field of construction materials, Xu et al. [155] developed a quaternary binder by incorporating AS into a ternary GBFS+SS+FDG matrix. The resulting formulation enhanced dissolution of the GBFS glass phase, accelerated hydration reactions, and improved early strength, thereby overcoming the delayed setting and low early strength typically observed in conventional ternary systems. Xu et al. [156] further extended this approach by combining AS, SS, GBFS, and FDG with iron-ore tailings and waste rock aggregates to produce a marine concrete composed entirely of industrial waste, demonstrating a promising route for comprehensive resource valorization.

In mine backfilling applications, Zhang et al. [157] proposed a ternary blend containing 35% SS, 50% GBFS, and 15% FDG. The binder paste exhibited a favorable strength development profile, with UCS of 6.69, 12.05, 16.36, and 18.37 MPa at 3, 7, 28, and 180 days, respectively. From a mechanistic perspective, Hao et al. [158] conducted a multi-scale characterization study to examine the hydration synergy in high SS content systems. Their findings indicated that optimal binder performance—with a 28-day compressive strength of approximately 38 MPa—was achieved when the mass ratios of SS:cement:GBFS:DG were in the range of 50–62:10:20–40:8–12. This improvement was attributed to a tri-coupled "nucleation–ionic–bond-energy" mechanism operating within the quaternary binder system (Figure 8a) [159–162]. Specifically: (i) early hydration of OPC releases Ca^{2+}, OH^-, and C–S–H nuclei, which establish an initial reaction framework and maintain a persistently alkaline environment; (ii) under these high-pH conditions, DG rapidly forms acicular AFt and facilitates the depolymerization of glassy phases in both GBFS and SS, thereby releasing reactive silicate and aluminate species; (iii) the dissolved Si and Al from SS and GBFS subsequently participate in the formation of abundant C–S–H, which drives continued strength development during mid- to late-stage curing. As shown in Figure 8b, at 7 days, a skeletal framework composed of intergrown AFt needles and C–S–H gel is evident; by 28 d, this framework

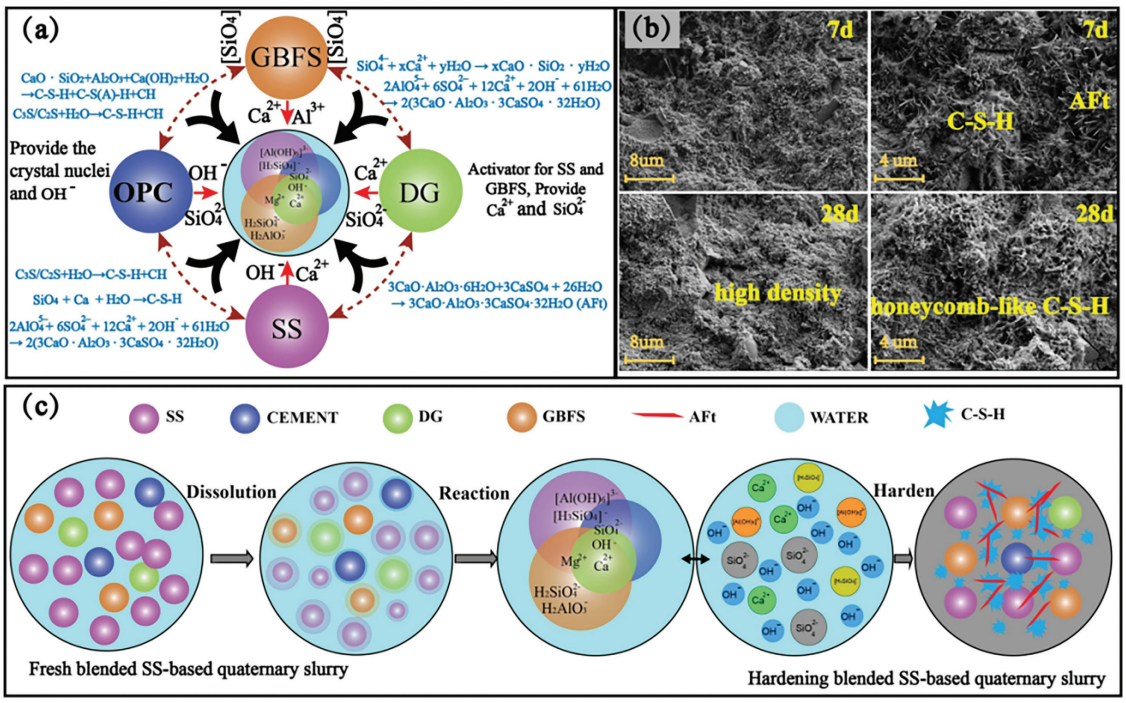

8 (a) Synergistic effects between SS, GBFS, OPC, and DG [159–162]; (b) Microscopic morphology and composition; (c) Hydration and hardening mechanism analysis of the system

evolves into a dense, honeycomb-like C–S–H network interlaced with AFt, substantially reducing porosity and enhancing microstructural integrity. As illustrated by the schematic hydration sequence in Figure 8c, the binder system progresses through distinct stages of dissolution, reaction, and hardening—ultimately forming a coordinated "skeleton–filling" microarchitecture jointly constructed by C–S–H and AFt phases. This continuous and coupled reaction pathway ensures effective integration of early nucleation processes with later-stage matrix densification, thereby significantly improving the mechanical performance of SS-based composite binders.

4.2 SS + FA based cementitious systems

Due to its high calcium content but relatively low levels of silicon and aluminum, SS benefits significantly from the incorporation of supplementary silicon and aluminum sources such as FA. This supplementation helps to optimize the Ca/Si and Ca/Al ratios within the binder matrix. In the alkaline environment generated by SS hydrolysis, reactive calcium and aluminum species released from FA participate in hydration reactions to form C–S–H and C–A–H gels [163, 164]. These reaction products not only enhance mechanical strength but also mitigate expansion associated with SS, thereby improving the structural stability of the composite system [165–168]. When the W/B ratio is maintained at 0.40 and FA and SS are used in a 1:1 mass ratio to replace 40% of OPC, the hardened paste demonstrates optimal performance [169]. Additional studies have shown that partially replacing FA (20%) with high-calcium SS in a binary geopolymer matrix improves UCS, enhances tensile behavior, and reduces microcracking [170, 171].

Compared to binary SS+FA systems, ternary systems incorporating GBFS exhibit superior compressive and tensile strengths, faster early-age strength development, lower shrinkage, and enhanced chemical resistance [172–174]. Optimal performance has been reported for blends containing approximately 7.5–11.5% SS, 31.5–35.5% GBFS, and 55.5–58.5% FA, which balance strength and strain capacity effectively [175–177]. Duan et al. [22, 178] investigated a fully industrial-waste ternary binder composed of SS, ultrafine FA, and DG in a mass ratio of 70:20:10. This system achieved a 28-day UCS of 39.6 MPa, along with excellent water resistance, freeze–thaw durability, and abrasion resistance.

In the context of mine backfilling, a mix design containing 12% FA, 15% SS, and 10% DG demonstrated good flowability. The UCS reached 0.58 MPa at 3 days and 3.24 MPa at 28 days, while yield stress decreased by 35.1–64.9% [179]. The hydration process of SS+FA+DG ternary binders can be divided into five sequential stages (Figure 9): (i) hydrolysis of SS, controlled by particle size, crystallite size, and crystallinity [180]; (ii) formation of CH from liberated Ca^{2+} and OH^-, and alkaline activation of FA, releasing $H_2SiO_4^{2-}$ and $H_2AlO_3^-$; (iii) precipitation of C–S–H from Ca^{2+} and $H_2SiO_4^{2-}$ and formation of microcrystalline AFt from SO_4^{2-}, $H_2AlO_3^-$, and Ca^{2+}; (iv) rapid growth of C–S–H and AFt, encapsulating unreacted particles; and (v) nucleation and crystallization of hydration products on particle surfaces, forming an interwoven reaction network.

In more complex quaternary binder systems, the combined incorporation of FA, GBFS, SS, and DG has been shown to produce materials with excellent mechanical properties, improved workability, and enhanced environmental performance [181–183]. The spherical morphology of FA contributes to improved particle packing and reduced water demand, while imparting a "ball-bearing" lubrication effect that significantly enhances rheology and flowability [184]. As a representative

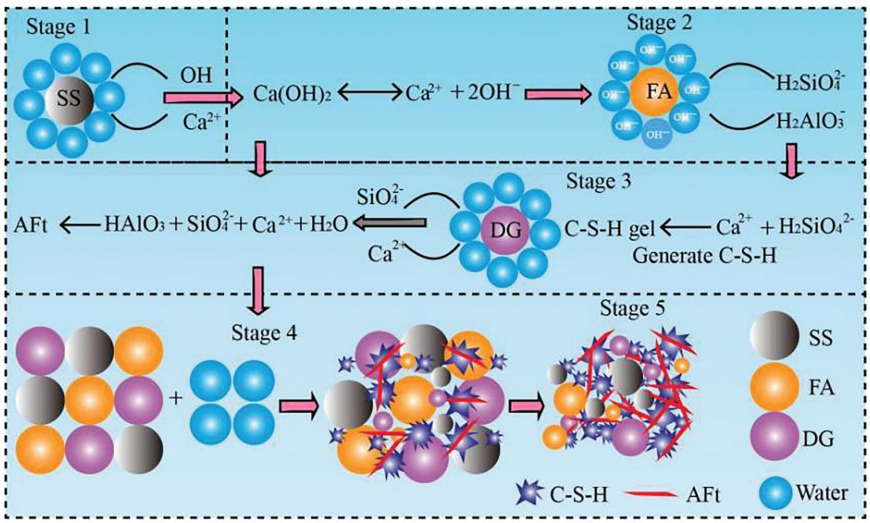

Figure 9 Reaction process and hydration mechanism of SS+FA+DG cementing system [180]

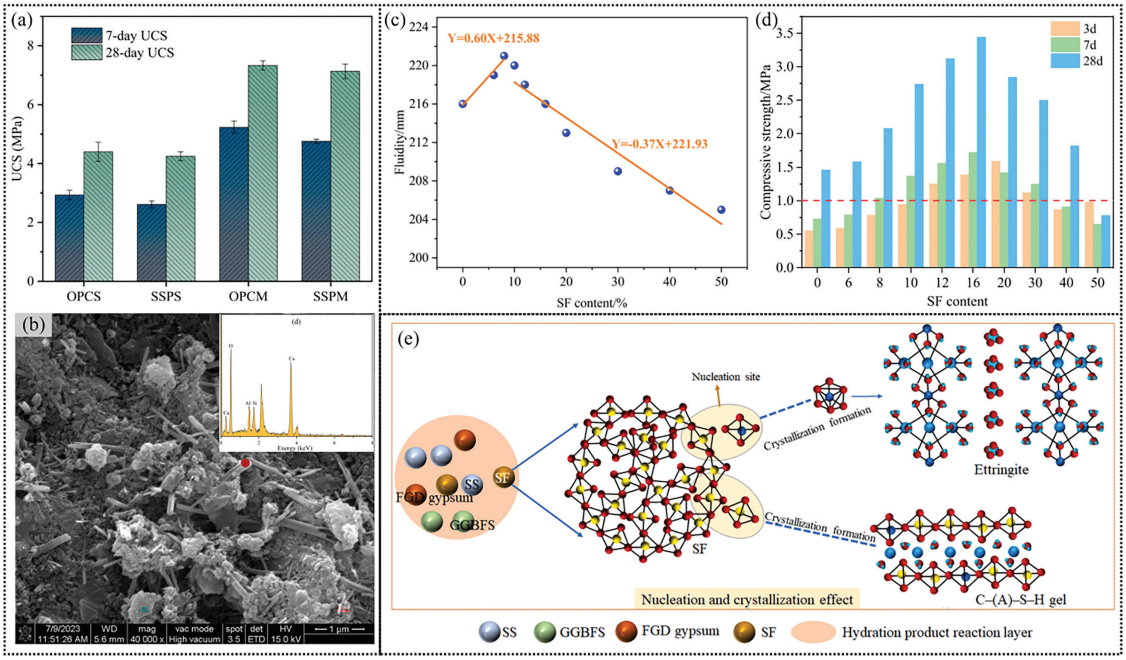

10 **Performance and synergistic mechanism of the SS + SF composite binder**

example, a cemented ultra-fine tailings backfill comprising 5–10% SS, 5–10% FA, 16–22% CS, 0–3% DG, and 40–74% GBFS—combined with ultra-fine tailings (d_{50} = 10.84 µm)—achieved 28-day UCS that were 10.80–44.89% higher than those of cement-based controls. These improvements indicate not only strong long-term strength potential but also the formation of a refined and denser microstructure [185].

4.3 SS + SF based cementitious systems

The limited reactivity and expansion potential of SS have restricted its widespread utilization in cementitious systems. In contrast, SF, characterized by a high content of amorphous SiO_2, elevated pozzolanic activity, ultrafine particle size, and large specific surface area, significantly contributes to the development of a denser and more compact microstructure in such systems [186, 187]. During the hydration of SS, the reaction of C_2S and C_3S phases releases CH, creating a highly alkaline environment that activates the latent pozzolanic reactivity of SF. This activation promotes secondary hydration reactions, accelerating the formation of key hydration products such as C–S–H gel and AFt. The synergistic interaction between SS and SF thereby enhances both the mechanical strength and the microstructural integrity of the binder matrix [188, 189].

In a study on blended mineral admixtures incorporating both SS and SF, Li et al. [185] co-ground composite binders with 8% and 16% SF. The SF particles were uniformly agglomerated onto the surfaces of SS, thereby improving interfacial bonding with C–S–H gel [190]. This enhanced interfacial interaction led to substantial improvements in the long-term mechanical performance of the composites, as well as increased resistance to chloride ion penetration, carbonation, and sulfate attack (Figure 10a,b). Deng et al. [191] applied a D-optimal design approach to optimize a ternary binder system composed of SS, SF, and OPC, identifying the optimal formulation as 16.238% SS and 1.917% SF. Experimental results demonstrated that SF effectively refined the pore structure and improved matrix compactness, resulting in compressive strength gains of up to 62.6% between 7 and 28 days.

In a fully solid-waste-based binder system comprising SF, GBFS, SS, and DG, Zhang et al. [192] reported that incorporating 16% SF yielded superior performance across various parameters, including UCS, drying shrinkage, and electrical resistivity (Figure 10c,d). These enhancements were attributed to a "triple-action mechanism" of SF at the microscale. First, the micro-filler effect of SF enabled it to fill interstitial voids between solid waste particles such as SS, leading to the formation of a denser particle skeleton and improved early-age strength. The spherical morphology of SF also reduced interparticle friction, thereby decreasing plastic viscosity and enhancing rheological behavior [157, 193, 194]. Second, the high concentration of reactive silica in SF—uniformly agglomerated onto SS surfaces—provided abundant nucleation sites for hydration, functioning via a seeding effect (Figure 10e). This not only accelerated hydration kinetics but also promoted pozzolanic reactions with Ca^{2+}, forming additional C–S–H gel. Furthermore, the pozzolanic activity of SF facilitated the secondary

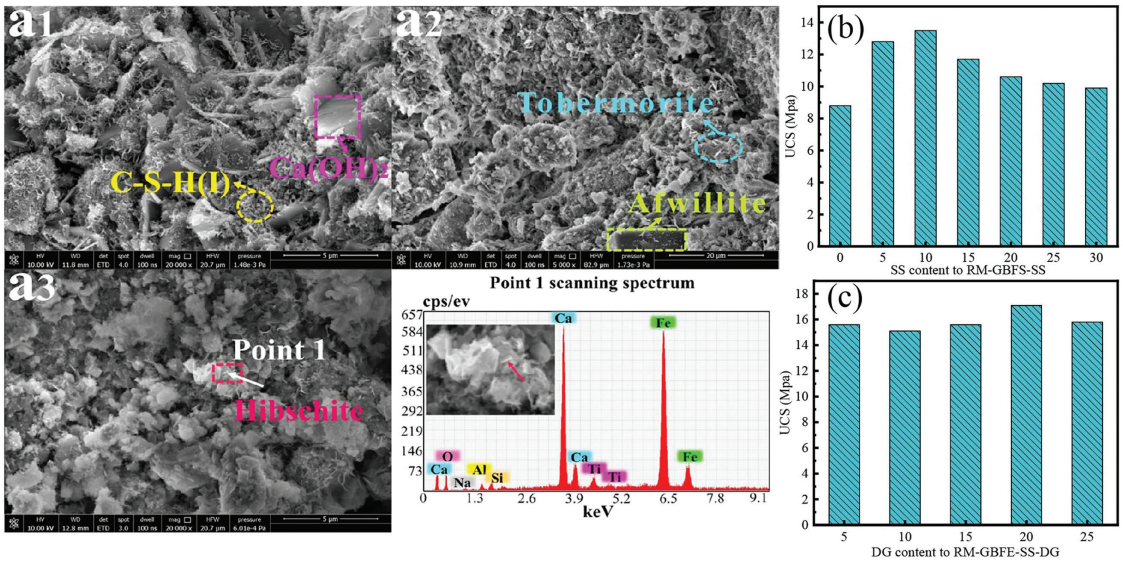

11 Performance and reaction mechanism analysis of a SS/RM based cementitious system [204–207]

hydration of CH released from SS, resulting in further C–S–H formation and improved microstructural continuity between SS particles and the binding matrix. Finally, SF contributed to pore structure refinement by filling harmful capillary pores, thereby enhancing matrix densification and improving overall durability of the hardened binder [195–197].

4.4 SS + RM based cementitious systems

The integration of RM with SS can significantly enhance the mechanical performance of cementitious materials while simultaneously facilitating the high-value utilization of industrial solid waste. This synergy supports the development of sustainable construction materials [198, 199]. Owing to its distinctive chemical composition—rich in aluminum and low in silicon—RM complements the highly reactive calcium phases present in SS. This chemical compatibility provides a theoretical basis for optimizing the Ca/Al ratio in the composite binder system, thereby improving its overall performance. Incorporating additional solid waste materials, such as FA, iron tailings, GBFS, and FGD—into the binary SS + RM system diversifies hydration pathways, enhances system reactivity, accelerates hydration kinetics, and improves microstructural densification [200–202]. For instance, Kumar et al. [203] developed a multi-component binder composed of RM, CS, SS, GBFS, and FGD, which achieved a one-day UCS of 16.3 MPa—significantly surpassing that of conventional Portland and sulfoaluminate cements. This high early strength was primarily attributed to the rapid hydration of calcium sulfoaluminate phases in the presence of gypsum, as well as the substantial β-C_2S content, which contributed to later-age strength development.

Moreover, the synergistic coupling of multiple solid waste components intensifies chemical interactions among constituents, refines the mineralogical composition of hydration products (Figure 11a), and substantially enhances both the comprehensive mechanical performance and environmental adaptability of the binder system [204, 205]. In a ternary binder composed of GBFS, RM, and SS, mechanical strength was found to be optimal when SS content was maintained at 10% (Figure 11b). This improvement was primarily due to the rapid hydration of active mineral phases in SS—including C_2S, C_3S, and C_2F—under alkaline conditions, which facilitated the formation of abundant C–S–H gels and reinforced the hardened matrix [206]. However, increasing the SS content beyond 20% led to a decline in mechanical performance. This reduction was attributed to the accumulation of inert mineral phases (e.g., RO phases and calcite) and the limited short-term reactivity of C_2S, which hindered the continuation of cementitious reactions [207].

The incorporation of 20% FGD into the ternary system introduced additional reaction pathways, markedly enhancing both early- and late-age UCS (Figure 11c). This improvement is attributed to the complex chemical synergies among the multi-component solid wastes involved. Specifically, the high alkalinity of RM activated the latent reactivity of SS, while GBFS provided a rich reservoir of reactive silica and calcium. The FGD contributed SO_4^{2-} and Ca^{2+}, promoting the formation of stable hydration products such as AFt. These synergistic interactions mobilized otherwise inert components in both RM and SS, thereby facilitating sustained strength development over time [208, 209]. Ultimately, the generation of strength-bearing hydration phases—such as C–S–A–H, N–C–S–A–H, and AFt—resulted in a

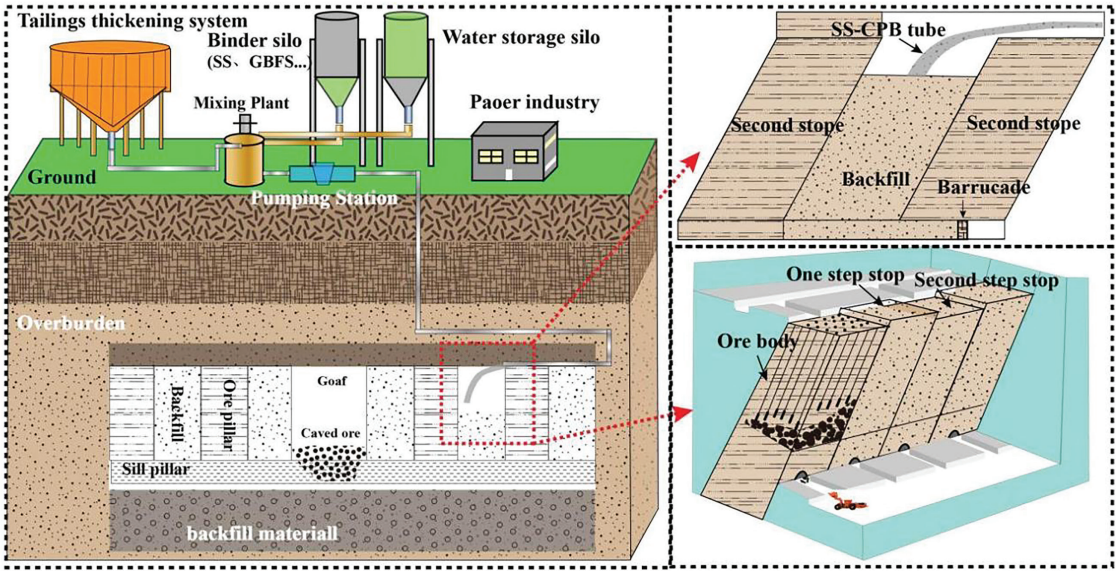

12 Application of SS based tailings backfill materials in cut-and-fill mining

pronounced enhancement in both the mechanical performance and volumetric stability of the composite binder system [210, 211].

5 Analysis of the application prospects of SS-based cementitious materials

5.1 Application potential of steel slag based mine backfill materials

Amid growing demand for mineral resources and increasingly stringent ecological and environmental regulations, the green transformation of the mining industry and the circular utilization of resources have emerged as core themes in sustainable development. Compared to structural concrete, cemented paste backfill (CPB) typically requires lower performance thresholds, making it particularly suitable for incorporating industrial solid wastes that continue to face technical barriers in conventional construction applications. Utilizing tailings, SS, and other metallurgical residues for underground backfilling not only contributes to controlling surface subsidence and improving mining safety, but also promotes waste reduction and resource valorization—key objectives aligned with the principles of green mining and sustainable extraction.

Steel slag offers notable engineering advantages in the design of mine backfill systems (Figure 12). Conventional CPB formulations are often associated with high energy consumption, substantial carbon emissions, and elevated costs—factors that conflict with China's "dual carbon" strategy and the global push toward low-carbon metallurgical processes [212–214]. The development of low-carbon cementitious materials derived from industrial by-products such as SS and GBFS can substantially reduce the carbon footprint and material costs associated with mine backfilling, while simultaneously advancing the high-value utilization of solid industrial wastes. This approach also supports resource recycling and ecological restoration in mining-impacted regions.

As mining operations extend into deeper geological formations, working faces are increasingly exposed to dynamic hazards such as roadway deformation, rock bursts, and roof collapses—all of which pose significant safety threats [215, 216]. SS-based cemented paste backfill (SS-CPB) can serve as a flexible medium that effectively absorbs and redistributes stress from surrounding rock masses, thereby mitigating ground pressure release and slowing energy dissipation. Experimental findings have shown that increasing SS content enhances the ductility of the backfill material, as evidenced by higher peak strain and improved post-peak strength characteristics [217]. Under impact-induced ground pressure conditions, SS-CPB exhibits the ability to support overburden loads and improve stress transfer across the ore body, thereby reducing the likelihood of dynamic failures. In addition to its mechanical performance, SS-CPB is distinguished by its low heat of hydration—a critical advantage over CPB. The hydration process of SS-CPB releases significantly less thermal energy, thereby lowering the internal temperature of the fill body. Moreover, during transport and placement from the surface to subsurface voids, SS-CPB can absorb considerable amounts of heat, contributing to temperature moderation within the stope environment [218, 219].

Mineral carbonation has further been demonstrated to significantly enhance the mechanical strength and durability of SS-CPB systems [220, 221]. The use of carbonated SS in backfill

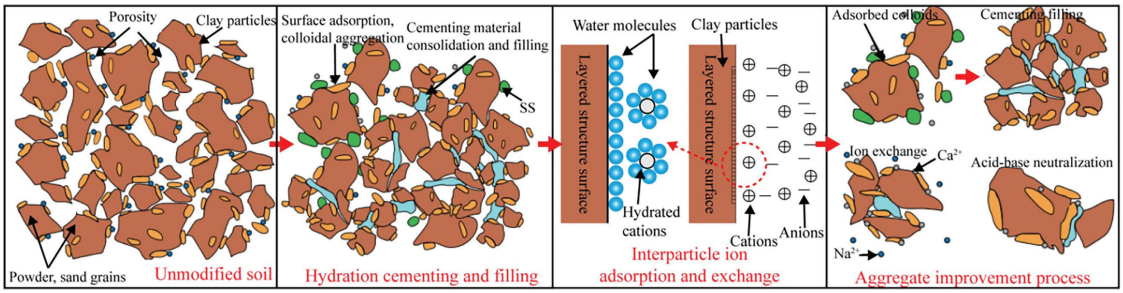

13 Mechanism of chemical stabilization of expansive clay using SS powder [224–226]

applications provides a more environmentally friendly, lower-carbon, and technically efficient solution for modern mining operations. By optimizing carbonation reaction conditions and exploring synergistic effects between various industrial residues and CO_2, it is possible to further diversify and improve the performance of backfill materials [112, 222]. These advances hold substantial promise for supporting ecological restoration and long-term sustainability in mining regions.

5.2 Stabilization of expansive clay using ground steel slag powder

Expansive clays are highly vulnerable to deformation, slope instability, and landslides under prolonged hot and humid conditions, posing serious risks to infrastructure stability and safety. Owing to its distinct mineralogical composition—particularly the abundance of reactive components such as CaO and Fe_2O_3—SS can interact with soil moisture and clay particles through ion exchange and cementitious reactions. These processes generate stable gel-like products that fill microfissures and bind soil particles, thereby increasing soil density and enhancing structural integrity. As a result, key geotechnical properties of expansive soils—including plasticity, free swell ratio, unconfined compressive strength, and drainage performance—can be markedly improved [223, 224]. The use of granulated steel slag powder for soil stabilization not only aligns with low-carbon and environmentally sustainable engineering practices, but also enables the high-value utilization of industrial solid waste while reducing overall treatment costs.

The physical stabilization mechanisms of SS primarily involve fine-particle filling, enhancement of interparticle friction, and skeletal support provided by coarse particles [225]. Fine SS particles effectively occupy pore spaces between soil grains, thereby increasing compaction and reducing deformability. The increased frictional resistance among soil and slag particles enhances aggregate cohesion and shear strength. Simultaneously, larger SS particles, due to their high stiffness and strength, contribute to overall load-bearing capacity and mitigate settlement potential, further improving soil mechanical performance. From a chemical perspective, SS is predominantly composed of CaO, Fe_2O_3, and SiO_2, with total reactive mineral content reaching up to 80%. Upon hydration, these oxides react to form cementitious phases such as C–S–H, C–A–H, and minor amounts of AFt. As illustrated in Figure 13, specific components in SS also participate in ion exchange and adsorption reactions with clay minerals, generating secondary gels and hydration products. These phases fill residual pores within the soil matrix, substantially enhancing compactness, durability, and long-term stability of stabilized expansive clays [226–228].

It should be noted that applying SS-based cementitious materials in soil stabilization, or expansive soil improvement requires careful assessment of potential leaching from trace metals (e.g., Cr, V, Mo, Mn, Cu, Zn, Pb) and their long-term environmental impact [229, 230]. Research shows that under high alkalinity, unstabilized SS may cause short-term release of certain metals or oxyanions [231, 232]. However, adding high Si/Al solid wastes (such as GBFS or FA) or additives like DG can immobilize metals into stable mineral phases through precipitation, adsorption, or chemical bonding, significantly reducing leaching risk [233, 234].

6 Conclusions

Steel slag is commonly categorized by smelting route into BOFS, EAFS, and LFS. Among these, BOFS and EAFS together account for >95% of global production, making them the principal targets for recycling and utilization. BOFS typically exhibits high CaO contents (40–55%), total Fe of 13.6–29.49%, and high basicity (CaO/SiO_2 ≈ 2.3–3.5). By contrast, EAFS generally contains lower CaO (25–35%), higher total Fe (22–35%), and elevated SiO_2 (12–20%), features that confer improved volumetric stability and lower alkalinity. Notwithstanding its chemical potential, SS tends to be weakly reactive owing to its predominantly crystalline microstructure. The presence of hard, poorly reactive phases—such as RO solid solutions and magnetite (Fe_3O_4)—together with

metallic iron, results in high Mohs hardness and poor grindability. To mitigate these drawbacks, gypsum, calcium chloride, and ethanol are frequently employed as grinding aids.

To overcome low reactivity and latent instability, a suite of activation strategies has been investigated, including mechanical, chemical, thermal, carbonation, and online reconstruction activation approaches. Mechanical activation primarily increases fineness and surface energy, yielding modest but reliable gains in hydration. Chemical activation adjusts phase assemblages through targeted admixtures, though it can entail higher energy demand and environmental burdens associated with reagent recovery. Thermal activation markedly enhances reactivity, but requires careful energy–performance optimization. Carbonation activation has attracted particular interest because it can accelerate hydration and early strength development with a reduced carbon footprint, offering potential synergies with CO_2 utilization. Finally, *in-situ* modification tailors the mineralogy to generate highly reactive phases, thereby improving hydration kinetics and dimensional stability; although still developing, this route shows strong promise for solid-waste valorization and low-carbon construction materials.

A complementary strategy is to exploit cross-waste synergism to enhance the mechanical performance, microstructural compactness, and environmental robustness of SS-based binders. Based on dominant chemistries, solid wastes can be grouped as high-calcium, high-alkaline, high-sulfate, and silica–alumina-rich classes. By regulating the availability of Ca, Si, Al, and SO_4^{2-} and controlling system pH, these additives promote SS dissolution and activate the latent reactivity of SS. In practice, GBFS, FGD, FA, SF, and RM have demonstrated robust synergistic effects with SS and are already deployed in engineering applications, thereby advancing resource efficiency.

The application prospects of SS-based binders are particularly evident in mine backfilling and expansive-soil stabilization. For mine backfilling, the intrinsic reactivity of SS contributes to strength and stability while offering low hydration heat and reduced embodied carbon, consistent with sustainable mining and site rehabilitation. For expansive soils, SS powder enhances compactness and strength via ion exchange and cementitious bonding, leading to improved plasticity indices and shear resistance. Collectively, these pathways align with low-carbon, eco-efficient development goals and provide high-value utilization routes for industrial solid waste.

Acknowledgement

Not applicable.

Funding Statement

This research was funded by the National Natural Science Foundation of China (Nos. 52408276 and 52308316), the China Postdoctoral Science Foundation (2025M771816), the Fudamental Research Funds for the Central Universities, CHD (No. 300102265303).

Author Contributions

Jianshuai Hao: formal analysis, methodology, writing—original draft. Kuizhen Fang: conceptualization, methodology. Zihan Zhou: writing—review and editing, supervision, funding acquisition. Shiyu Zhuang: writing—review and editing, supervision, funding acquisition. All authors reviewed the results and approved the final version of the manuscript.

Availability of Data and Materials

The experimental data used to support the findings of this study are included in the article.

Ethics Approval

Not applicable.

Conflicts of Interest

The authors declare no conflicts of interest to report regarding the present study.

Nomenclature

Symbol	Meaning
SS	Steel slag
BOFS	Basic oxygen furnace slag
EAFS	Electric arc furnace slag
LFS	Ladle furnace slag
PDG	Phosphogypsum
AR	Alkali residue
DA	Desulfurization ash
RM	Red mud
f-CaO	Free CaO/free lime
f-MgO	Free MgO/periclase
C-(A)-S-H	Calcium (alumino)silicate hydrate
CPB	Cemented paste backfill
GBFS	Granulated blast furnace slag
FDA	Flue-gas desulfurization ash
OPC	Ordinary Portland cement
FA	Fly ash
CGS	Coal gasification slag
CS	Carbide slag
SEM	Scanning electron micrographs
SF	Silica fume
AOT	Aluminous ore tailings
LS	Lithium slag
EMR	Electrolytic manganese slag
MK	Metakaolin

REFERENCES

[1] World Steel Association. Steel industry co-products. Brussels, Belgium: World Steel Association; 2020.
[2] Feng YH, Zhang Z, Gao J, Feng GP, Qiu L, Feng DL, et al. Research status of centrifugal granulation, physical heat recovery and resource utilization of blast furnace slags. J Anal Appl Pyrolysis. 2021;157:105220. doi:10.1016/j.jaap.2021.105220.
[3] Chen J, Xing Y, Wang Y, Zhang W, Guo Z, Su W. Application of iron and steel slags in mitigating greenhouse gas emissions: a review. Sci Total Environ. 2022;844:157041. doi:10.1016/j.scitotenv.2022.157041.
[4] Martins ACP, Franco de Carvalho JM, Costa LCB, Andrade HD, de Melo TV, Ribeiro JCL, et al. Steel slags in cement-based composites: an ultimate review on characterization, applications and performance. Constr Build Mater. 2021;291:123265. doi:10.1016/j.conbuildmat.2021.123265.
[5] World Steel Association. December 2022 crude steel production and 2022 global crude steel production totals. Brussels, Belgium: World Steel Association; 2023.
[6] Sun R. Study on desulfurized ash-steel slag composite cementing material and its interfacial transition zone of concrete [dissertation]. Beijing, China: China University of Mining and Technology (Beijing); 2023. (In Chinese).
[7] Zhiyan Consulting. Report on market research and investment prospect planning of China steel slag treatment industry 2024–2030. Beijing, China: Zhiyan Consulting; 2024. (In Chinese).
[8] World Steel Association. World crude steel production [Internet]. World Steel Association; 2020 [cited 2020 Mar 15]. Available from: https://www.worldsteel.org/.
[9] Intelligence Research Group. Market research analysis and investment prospect assessment report on china steel slag cement industry, 2022–2028. Beijing, China: Zhiyan Consulting; 2022. (In Chinese).
[10] Matsuura H, Yang X, Li G, Yuan Z, Tsukihashi F. Recycling of ironmaking and steelmaking slags in Japan and China. Int J Miner Metall Mater. 2022;29(4):739–49. doi:10.1007/s12613-021-2400-5.
[11] Nunes VA, Borges PHR. Recent advances in the reuse of steel slags and future perspectives as binder and aggregate for alkali-activated materials. Constr Build Mater. 2021;281:122605. doi:10.1016/j.conbuildmat.2021.122605.
[12] Najm O, El-Hassan H, El-Dieb A. Ladle slag characteristics and use in mortar and concrete: a comprehensive review. J Clean Prod. 2021;288:125584. doi:10.1016/j.jclepro.2020.125584.
[13] Hao J, Zhou Z, Chen Z, Che Z. Failure behavior of rock and steel slag cemented paste backfill composite structures under uniaxial compression: effects of interface angle and steel slag content. J Cent South Univ. 2025;32(7):2679–95. doi:10.1007/s11771-025-6012-5.
[14] Sun R, Fang C, Zhang H, Ling Y, Feng J, Qi H, et al. Chemo-mechanical properties of alkali-activated slag/fly ash paste incorporating white mud. Constr Build Mater. 2021;291:123312. doi:10.1016/j.conbuildmat.2021.123312.
[15] Zhao W, Yan B, Li P, Chen D, Guo H, Liu Z, et al. Interface behavior and oxidation consolidation mechanism of titanium-bearing iron sand particles with ball-milling pretreatment. Powder Technol. 2022;396:366–77. doi:10.1016/j.powtec.2021.11.008.
[16] Singh SK, Jyoti, Vashistha P. Development of newer composite cement through mechano-chemical activation of steel slag. Constr Build Mater. 2021;268(3):121147. doi:10.1016/j.conbuildmat.2020.121147.
[17] Chen Z, Li R, Zheng X, Liu J. Carbon sequestration of steel slag and carbonation for activating RO phase. Cem Concr Res. 2021;139:106271. doi:10.1016/j.cemconres.2020.106271.
[18] Zhuang S, Wang Q. Inhibition mechanisms of steel slag on the early-age hydration of cement. Cem Concr Res. 2021;140:106283. doi:10.1016/j.cemconres.2020.106283.
[19] Du H, Xu D, Li X, Li J, Ni W, Li Y, et al. Application of molten iron desulfurization slag to replace steel slag as an alkaline component in solid waste-based cementitious materials. J Clean Prod. 2022;377:134353. doi:10.1016/j.jclepro.2022.134353.
[20] Zulhan Z, Agustina N. A novel utilization of ferronickel slag as a source of magnesium metal and ferroalloy production. J Clean Prod. 2021;292:125307. doi:10.1016/j.jclepro.2020.125307.
[21] Li K, Li X, Yao J, Sun Q, Xue H, Du C. Innovative synthesis of low-carbon cemented backfill materials through synergistic activation of solid wastes: an integrated assessment of economic and environmental impacts. Case Stud Constr Mater. 2024;20:e03203. doi:10.1016/j.cscm.2024.e03203.
[22] Duan S, Liao H, Cheng F, Song H, Yang H. Investigation into the synergistic effects in hydrated gelling systems containing fly ash, desulfurization gypsum and steel slag. Constr Build Mater. 2018;187:1113–20. doi:10.1016/j.conbuildmat.2018.07.241.
[23] Wang Y, Kong Q, Xie X, Lin L, Cui H, Long W, et al. Optimizing curing conditions for high-volume steel slag composites: gbfs synergy, microstructural refinement, and strength enhancement. Constr Build Mater. 2025;491:142777. doi:10.1016/j.conbuildmat.2025.142777.
[24] Muhmood L, Vitta S, Venkateswaran D. Cementitious and pozzolanic behavior of electric arc furnace steel slags. Cem Concr Res. 2009;39(2):102–9. doi:10.1016/j.cemconres.2008.11.002.
[25] Yin X, Ma L, Li K, Du W, Hou P, Dai Q, et al. Preparation of phosphogypsum-based cemented paste backfill and its environmental impact based on multi-source industrial solid waste. Constr Build Mater. 2023;404:133314. doi:10.1016/j.conbuildmat.2023.133314.
[26] Wan J, Han T, Li K, Shu S, Hu X, Gan W, et al. Effect of phosphogypsum based filler on the performance of asphalt mortar and mixture. Materials. 2023;16(6):2486. doi:10.3390/ma16062486.
[27] Pan SY, Adhikari R, Chen YH, Li P, Chiang PC. Integrated and innovative steel slag utilization for iron reclamation, green material production and CO_2 fixation via accelerated carbonation. J Clean Prod. 2016;137:617–31. doi:10.1016/j.jclepro.2016.07.112.
[28] Zhang Y, Yu L, Cui K, Wang H, Fu T. Carbon capture and storage technology by steel-making slags: recent progress and future challenges. Chem Eng J. 2023;455:140552. doi:10.1016/j.cej.2022.140552.
[29] Jiang A, Liu W, Fan J. Application and research on hydration mechanism and activation of steel slag. China Water Transp. 2022;22:159–60. (In Chinese).
[30] Yildirim IZ. Long-term and accelerated swelling of steel slag-glass powder and steel slag-fly ash mixtures as sustainable geo-materials. J Clean Prod. 2024;467:142768. doi:10.1016/j.jclepro.2024.142768.
[31] Carvalho VR, Costa LCB, da Fonseca Elói FP, da Silva Bezerra AC, de Carvalho JMF, Peixoto RAF. Performance of low-energy steel slag powders as supplementary cementitious materials. Constr Build Mater. 2023;392:131888. doi:10.1016/j.conbuildmat.2023.131888.
[32] Cárdenas Balaguera CA, Gómez Botero MA. Characterization of steel slag for the production of chemically bonded phosphate ceramics (CBPC). Constr Build Mater. 2020;241:118138. doi:10.1016/j.conbuildmat.2020.118138.
[33] Wang Y, Suraneni P. Experimental methods to determine the feasibility of steel slags as supplementary cementitious materials. Constr Build Mater. 2019;204:458–67. doi:10.1016/j.conbuildmat.2019.01.196.
[34] Maghool F, Arulrajah A, Suksiripattanapong C, Horpibulsuk S, Mohajerani A. Geotechnical properties of steel slag aggregates: shear strength and stiffness. Soils Found. 2019;59(5):1591–601. doi:10.1016/j.sandf.2019.03.016.
[35] Gómez-Casero MA, Bueno-Rodríguez S, Castro E, Eliche Quesada D. Alkaline activated cements obtained from ferrous and non-ferrous slags. Electric arc furnace slag, ladle furnace slag, copper slag and silico-manganese slag. Cem Concr Compos. 2024;147(1):105427. doi:10.1016/j.cemconcomp.2023.105427.
[36] Thwe KS, Ayawanna J, Mase LZ, Chaiyaput S. Utilization of ladle furnace slag and fly ash as partially replacement of cement. Clean Eng Technol. 2025;25:100910. doi:10.1016/j.clet.2025.100910.
[37] Costa LCB, Carvalho VR, Ferreira LC, Baeta BEL, Peixoto RAF. Utilizing steel slag to prolong the durability of reinforced concrete: corrosion resistance mechanisms. J Build Eng. 2024;98:111505. doi:10.1016/j.jobe.2024.111505.
[38] Shu K, Sasaki K. Occurrence of steel converter slag and its high value-added conversion for environmental restoration in China: a review. J Clean Prod. 2022;373:133876. doi:10.1016/j.jclepro.2022.133876.
[39] Bulatbekova D, Vashistha P, Kim HK, Pyo S. Effects of basic-oxygen furnace, electric-arc furnace, and ladle furnace slags on the hydration and durability properties of construction materials: a review. J Build Eng. 2024;92:109670. doi:10.1016/j.jobe.2024.109670.
[40] Fu S, Kwon EE, Lee J. Upcycling steel slag into construction materials. Constr Build Mater. 2024;444:137882. doi:10.1016/j.conbuildmat.2024.137882.
[41] Li T, Yang G, Chen H, Gu H, Li H. Basic properties and utilization of steel slag in different production stages and treatment processes. Bull Chin Ceram Soc. 2015;34(9):2619–23. (In Chinese).
[42] Chiang PC, Pan SY. Iron and steel slags. In: Carbon dioxide mineralization and utilization. Singapore: Springer Singapore; 2017. p. 233–52. doi:10.1007/978-981-10-3268-4_11.
[43] Hao J, Zhou Z, Chen Z, Zhao Z, Shen Y. Mechanical performance and damage mechanisms of steel slag-cement pasted backfill under high-temperature cured and cyclic static loading for deep-mining applications. J Mater Res Technol. 2025;35:5698–716. doi:10.1016/j.jmrt.2025.02.150.
[44] Mishra A, Lahoti M, Yang EH. Mitigating environmental impact by development of ambient-cured EAF slag and fly ash blended geopolymer via mix design optimization. Environ Sci Pollut Res Int. 2024;31(27):38908–25. doi:10.1007/s11356-023-26884-8.
[45] Pang L, Liao S, Wang D, An M. Influence of steel slag fineness on the hydration of cement-steel slag composite pastes. J Build Eng. 2022;57:104866. doi:10.1016/j.jobe.2022.104866.
[46] Wang Q, Shi M, Zhang Z. Hydration properties of steel slag under autoclaved condition. J Therm Anal Calorim. 2015;120(2):1241–8. doi:10.1007/s10973-015-4397-3.
[47] Zhao Y, Sun P, Chen P, Guan X, Wang Y, Liu R, et al. Component modification of basic oxygen furnace slag with C4AF as target mineral and application. Sustainability. 2021;13(12):6536. doi:10.3390/su13126536.
[48] Jonczy I, Grzesik B. Polymorphic transformations of dicalcium silicates in steel slags used in the production of road aggregates. Gospodarka Surowcami Miner Miner Resour Manag. 2022;2022:97–116. doi:10.24425/gsm.2021.139745.
[49] Carvalho SZ, Vernilli F, Almeida B, Demarco M, Silva SN. The recycling effect of BOF slag in the Portland cement properties. Resour Conserv Recycl. 2017;127:216–20. doi:10.1016/j.resconrec.2017.08.021.
[50] Hafez H, Kassim D, Kurda R, Silva RV, de Brito J. Assessing the sustainability potential of alkali-activated concrete from electric arc furnace slag using the ECO_2 framework. Constr Build Mater. 2021;281:122559. doi:10.1016/j.conbuildmat.2021.122559.
[51] Vashistha P, Park S, Pyo S. A review on sustainable fabrication of futuristic cementitious binders based on application of waste concrete powder, steel slags, and coal bottom ash. Int J Concr Struct Mater. 2022;16(1):51. doi:10.1186/s40069-022-00541-9.
[52] Guo X, Zeng M, Yu H, Lin F, Li J, Wang W, et al. Critical review for the potential analysis of material utilization from inorganic industrial solid waste. J Clean Prod. 2024;459:142457. doi:10.1016/j.jclepro.2024.142457.
[53] Dash A, Chanda P, Tripathy PK, Kumar N. A review on stabilization of ladle furnace slag-powdering issue. J Sustain Metall. 2022;8(4):1435–49. doi:10.1007/s40831-022-00597-7.
[54] Matalkah F, Ababneh A, Aqel R. Enhancement of the mechanical properties of mortar with low-quality steel slag through sodium sulfate activation: a path towards sustainable concrete. Eur J Environ Civ Eng. 2025;1–19. doi:10.1080/19648189.2025.2477059.
[55] Hao J, Zhou Z, Zhang L. Optimisation and mechanism of steel slag–cement based grouting for water ingress control. Case Stud Constr Mater. 2025;23:e05211. doi:10.1016/j.cscm.2025.e05211.
[56] Skaf M, Ortega-López V, Fuente-Alonso JA, Santamaría A, Manso JM. Ladle furnace slag in asphalt mixes. Constr Build Mater. 2016;122:488–95. doi:10.1016/j.conbuildmat.2016.06.085.
[57] Yi Y, Ma W, Sidike A, Ma Z, Fang M, Lin Y, et al. Synergistic effect of hydration and carbonation of ladle furnace aslag on cementitious substances. Sci Rep. 2022;12(1):14526. doi:10.1038/s41598-022-18215-7.
[58] Song Q, Guo MZ, Wang L, Ling TC. Use of steel slag as sustainable construction materials: a review of accelerated carbonation treatment. Resour Conserv Recycl. 2021;173:105740. doi:10.1016/j.resconrec.2021.105740.
[59] Yang C, Xie J, Wu S, Amirkhanian S, Zhou X, Kong D, et al. Revelation and characterization of selective absorption behavior of bitumen to basic oxygen furnace slag. Constr Build Mater. 2020;253:119210. doi:10.1016/j.conbuildmat.2020.119210.
[60] Espinosa AB, Revilla-Cuesta V, Skaf M, Serrano-López R, Ortega-López V. Strength performance of low-bearing-capacity clayey soils stabilized with ladle furnace slag. Environ Sci Pollut Res Int. 2023;30(45):101317–42. doi:10.1007/s11356-023-29375-y.

[61] Hu J. Comparison between the effects of superfine steel slag and superfine phosphorus slag on the long-term performances and durability of concrete. J Therm Anal Calorim. 2017;128(3):1251–63. doi:10.1007/s10973-017-6107-9.
[62] Rosales J, Agrela F, Díaz-López JL, Cabrera M. Alkali-activated stainless steel slag as a cementitious material in the manufacture of self-compacting concrete. Materials. 2021;14(14):3945. doi:10.3390/ma14143945.
[63] Li J, Ni W, Wang X, Zhu S, Wei X, Jiang F, et al. Mechanical activation of medium basicity steel slag under dry condition for carbonation curing. J Build Eng. 2022;50:104123. doi:10.1016/j.jobe.2022.104123.
[64] Kaja AM, Schollbach K, Melzer S, van der Laan SR, Brouwers HJH, Yu Q. Hydration of potassium citrate-activated BOF slag. Cem Concr Res. 2021;140:106291. doi:10.1016/j.cemconres.2020.106291.
[65] Kriskova L, Pontikes Y, Cizer Ö, Mertens G, Veulemans W, Geysen D, et al. Effect of mechanical activation on the hydraulic properties of stainless steel slags. Cem Concr Res. 2012;42(6):778–88. doi:10.1016/j.cemconres.2012.02.016.
[66] Duan S, Liao H, Song H, Cheng F, Yang H. Performance improvement to ash-cement blocks by adding ultrafine steel slag collected from a supersonic steam-jet smasher. Constr Build Mater. 2019;212:140–8. doi:10.1016/j.conbuildmat.2019.03.320.
[67] Shi Y, Chen H, Wang J, Feng Q. Preliminary investigation on the pozzolanic activity of superfine steel slag. Constr Build Mater. 2015;82:227–34. doi:10.1016/j.conbuildmat.2015.02.062.
[68] Santos WF, Schollbach K, Melzer S, van der Laan SR, Brouwers HH. Quantitative analysis and phase assemblage of basic oxygen furnace slag hydration. J Hazard Mater. 2023;450:131029. doi:10.1016/j.jhazmat.2023.131029.
[69] Liu S, Li L. Influence of fineness on the cementitious properties of steel slag. J Therm Anal Calorim. 2014;117(2):629–34. doi:10.1007/s10973-014-3789-0.
[70] Thomas JJ, Ghazizadeh S, Masoero E. Kinetic mechanisms and activation energies for hydration of standard and highly reactive forms of β-dicalcium silicate (C_2S). Cem Concr Res. 2017;100:322–8. doi:10.1016/j.cemconres.2017.06.001.
[71] Wunderlich S, Schirmer T, Fittschen UEA. Investigation on vanadium chemistry in basic-oxygen-furnace (BOF) slags—a first approach. Metals. 2021;11(11):1869. doi:10.3390/met11111869.
[72] Mahieux PY, Aubert JE, Escadeillas G, Measson M. Quantification of hydraulic phase contained in a basic oxygen furnace slag. J Mater Civ Eng. 2014;26(4):593–8. doi:10.1061/(asce)mt.1943-5533.0000867.
[73] Zhao J, Wang D, Yan P, Li W. Comparison of grinding characteristics of converter steel slag with and without pretreatment and grinding aids. Appl Sci. 2016;6(11):237. doi:10.3390/app6110237.
[74] Zhu H, Ma M, He X, Zheng Z, Su Y, Yang J, et al. Effect of wet-grinding steel slag on the properties of Portland cement: an activated method and rheology analysis. Constr Build Mater. 2021;286:122823. doi:10.1016/j.conbuildmat.2021.122823.
[75] Liu PY, Li JG, Li GP, Tao MJ, Zhang X, Chao S, et al. Effect of glycerol mechanical excitation on the phase evolution and hydration activity of steel slag. ISIJ Int. 2024;64(6):1089–100. doi:10.2355/isijinternational.isijint-2023-424.
[76] Kim S, Yang J, Lee J, Poon CS, Moon J. Impact of triethanolamine on grinding and hydration performance of BOF steel slag blended cement. J Build Eng. 2025;101:111858. doi:10.1016/j.jobe.2025.111858.
[77] Sun X, Liu J, Zhao Y, Zhao J, Li Z, Sun Y, et al. Mechanical activation of steel slag to prepare supplementary cementitious materials: a comparative research based on the particle size distribution, hydration, toxicity assessment and carbon dioxide emission. J Build Eng. 2022;60:105200. doi:10.1016/j.jobe.2022.105200.
[78] Sajedi F, Razak HA. The effect of chemical activators on early strength of ordinary Portland cement-slag mortars. Constr Build Mater. 2010;24(10):1944–51. doi:10.1016/j.conbuildmat.2010.04.006.
[79] Shi J, Lan X, Yan C, Zhou X, Luo Z, Zhao S, et al. Upcycling of steel slag to activate persulfate for the degradation of chlortetracycline hydrochloride: performance and mechanism. Water Sci Technol. 2024;90(9):2660–72. doi:10.2166/wst.2024.358.
[80] Aydın S, Baradan B. Effect of activator type and content on properties of alkali-activated slag mortars. Compos Part B Eng. 2014;57:166–72. doi:10.1016/j.compositesb.2013.10.001.
[81] Gebregziabiher BS, Thomas R, Peethamparan S. Very early-age reaction kinetics and microstructural development in alkali-activated slag. Cem Concr Compos. 2015;55:91–102. doi:10.1016/j.cemconcomp.2014.09.001.
[82] Shi M, Wang Q, Zhou Z. Comparison of the properties between high-volume fly ash concrete and high-volume steel slag concrete under temperature matching curing condition. Constr Build Mater. 2015;98:649–55. doi:10.1016/j.conbuildmat.2015.08.134.
[83] Wang Q, Yang J, Yan P. Influence of initial alkalinity on the hydration of steel slag. Sci China Technol Sci. 2012;55(12):3378–87. doi:10.1007/s11431-012-4830-9.
[84] Yan F, Luo K, Ye J, Zhang W, Chen J, Ren X, et al. Leaching kinetics and dissolution model of steel slag in NaOH solution. Constr Build Mater. 2024;434:136743. doi:10.1016/j.conbuildmat.2024.136743.
[85] Wang Q, Yan P, Feng J. A discussion on improving hydration activity of steel slag by altering its mineral compositions. J Hazard Mater. 2011;186(2–3):1070–5. doi:10.1016/j.jhazmat.2010.11.109.
[86] Zhang S, Niu D. Hydration and mechanical properties of cement-steel slag system incorporating different activators. Constr Build Mater. 2023;363:129981. doi:10.1016/j.conbuildmat.2022.129981.
[87] Cristelo N, Coelho J, Miranda T, Palomo Á, Fernández-Jiménez A. Alkali activated composites—an innovative concept using iron and steel slag as both precursor and aggregate. Cem Concr Compos. 2019;103:11–21. doi:10.1016/j.cemconcomp.2019.04.024.
[88] Liu Q, Cho JW, Pereloma E. Editorial: advances in steel manufacturing and processing. Front Mater. 2021;8:708572. doi:10.3389/fmats.2021.708572.
[89] Guo X, Shi H. Modification of steel slag powder by mineral admixture and chemical activators to utilize in cement-based materials. Mater Struct. 2013;46(8):1265–73. doi:10.1617/s11527-012-9970-7.
[90] Fang Y, Su W, Zhang Y, Zhang M, Ding X, Wang Q. Effect of accelerated precarbonation on hydration activity and volume stability of steel slag as a supplementary cementitious material. J Therm Anal Calorim. 2022;147(11):6181–91. doi:10.1007/s10973-021-10914-z.
[91] Lv D, Yu Q, Shen M, Wang Y, Long H. Effect of modified steel slag on properties of rigid polyurethane foam. Int J Chem React Eng. 2025;23(1):1–12. doi:10.1515/ijcre-2024-0160.
[92] Zhang Z, Jia Z, Cao R, Wang W, Liu C, Gao Y, et al. Understanding the multiple actions of phosphoric acid-modified steel slag powder on early-age hydration of cement. Cem Concr Compos. 2024;150:105538. doi:10.1016/j.cemconcomp.2024.105538.
[93] Kong H, Luo K, Yong Z. Methacrylic acid *in situ* modified steel converter slag/natural rubber composites: resourceful utilization of steelmaking solid wastes. Waste Manag. 2024;180:36–46. doi:10.1016/j.wasman.2024.03.024.
[94] Chen G, Bian S, Gao J, Jin P, Wang R. Effect and mechanism of acetic acid to improve the hydration activity of steel slag. JOM. 2023;75(4):1079–88. doi:10.1007/s11837-022-05574-9.
[95] Yang C, Zhang Z, Yu H, Xu N, Rui Z, Chu H. Preparation and characterization of modified steel slag-based composite phase change materials. Int J Heat Fluid Flow. 2025;111:109666. doi:10.1016/j.ijheatfluidflow.2024.109666.
[96] Li Z, Xu G, Shi X. Reactivity of coal fly ash used in cementitious binder systems: a state-of-the-art overview. Fuel. 2021;301:121031. doi:10.1016/j.fuel.2021.121031.
[97] Luo S, Liu M, Yang L, Chang J, Yang W, Yan X, et al. Utilization of waste from alumina industry to produce sustainable cement-based materials. Constr Build Mater. 2019;229:116795. doi:10.1016/j.conbuildmat.2019.116795.
[98] Li Y, Tang X, Zhao HZ, Qi YP. Influence of calcination temperature on steel slag activity for preparing a gel material. J Iron Steel Res Int. 2025;32(7):1948–60. doi:10.1007/s42243-025-01452-1.
[99] Feng J, Sun J. A comparison of the 10-year properties of converter steel slag activated by high temperature and an alkaline activator. Constr Build Mater. 2020;234:116948. doi:10.1016/j.conbuildmat.2019.116948.
[100] Long Y, Shi Y, Lei YB, Xing HW, Li J, Zhang YZ. Study of modification of high temperature melting compound steel slag-fly ash. Adv Mater Res. 2011;291–294:1851–5. doi:10.4028/www.scientific.net/amr.291-294.1851.
[101] Fang K, Zhao J, Wang D, Wang H, Dong Z. Use of ladle furnace slag as supplementary cementitious material before and after modification by rapid air cooling: a comparative study of influence on the properties of blended cement paste. Constr Build Mater. 2022;314:125434. doi:10.1016/j.conbuildmat.2021.125434.
[102] Na H, Wang Y, Zhang X, Li J, Zeng Y, Liu P. Hydration activity and carbonation characteristics of dicalcium silicate in steel slag: a review. Metals. 2021;11(10):1580. doi:10.3390/met11101580.
[103] Zhuang S, Wang Q, Luo T. Effect of C12A7 in steel slag on the early-age hydration of cement. Cem Concr Res. 2022;162:107010. doi:10.1016/j.cemconres.2022.107010.
[104] Kravchenko E, Qin C, Lin Z, Ng CWW. Effect of polyvinyl alcohol on the CO_2 uptake of carbonated steel slag. Constr Build Mater. 2023;375:130761. doi:10.1016/j.conbuildmat.2023.130761.
[105] Chen Z, Li R, Liu J. Preparation and properties of carbonated steel slag used in cement cementitious materials. Constr Build Mater. 2021;283:122667. doi:10.1016/j.conbuildmat.2021.122667.
[106] Costa G, Polettini A, Pomi R, Stramazzo A. Leaching modelling of slurry-phase carbonated steel slag. J Hazard Mater. 2016;302:415–25. doi:10.1016/j.jhazmat.2015.10.005.
[107] Liu P, Mo L, Zhang Z. Effects of carbonation degree on the hydration reactivity of steel slag in cement-based materials. Constr Build Mater. 2023;370:130653. doi:10.1016/j.conbuildmat.2023.130653.
[108] Chen T, Xue Y, Zhao X, Liu J. Effects of EDTA on the accelerated carbonation behavior of steel slag used as cementitious materials. J Mater Cycles Waste Manag. 2023;25(3):1498–508. doi:10.1007/s10163-023-01622-x.
[109] Lothenbach B, Le Saout G, Gallucci E, Scrivener K. Influence of limestone on the hydration of Portland cements. Cem Concr Res. 2008;38(6):848–60. doi:10.1016/j.cemconres.2008.01.002.
[110] Thongsanitgarn P, Wongkeo W, Chaipanich A, Poon CS. Heat of hydration of Portland high-calcium fly ash cement incorporating limestone powder: effect of limestone particle size. Constr Build Mater. 2014;66:410–7. doi:10.1016/j.conbuildmat.2014.05.060.
[111] Liu P, Zhong J, Zhang M, Mo L, Deng M. Effect of CO_2 treatment on the microstructure and properties of steel slag supplementary cementitous materials. Constr Build Mater. 2021;309:125171. doi:10.1016/j.conbuildmat.2021.125171.
[112] Zhang X, Zhao J, Liu Y, Li J. Use of steel slag as carbonation material: a review of carbonation methods and evaluation, environmental factors and carbon conversion process. J CO2 Util. 2024;88:102947. doi:10.1016/j.jcou.2024.102947.
[113] Rushendra Revathy TD, Palanivelu K, Ramachandran A. Direct mineral carbonation of steelmaking slag for CO_2 sequestration at room temperature. Environ Sci Pollut Res Int. 2016;23(8):7349–59. doi:10.1007/s11356-015-5893-5.
[114] Moon EJ, Choi YC. Development of carbon-capture binder using stainless steel argon oxygen decarburization slag activated by carbonation. J Clean Prod. 2018;180:642–54. doi:10.1016/j.jclepro.2018.01.189.
[115] Salman M, Cizer Ö, Pontikes Y, Santos RM, Snellings R, Vandewalle L, et al. Effect of accelerated carbonation on AOD stainless steel slag for its valorisation as a CO_2-sequestering construction material. Chem Eng J. 2014;246:39–52. doi:10.1016/j.cej.2014.02.051.
[116] Santos RM, Ling D, Sarvaramini A, Guo M, Elsen J, Larachi F, et al. Stabilization of basic oxygen furnace slag by hot-stage carbonation treatment. Chem Eng J. 2012;203:239–50. doi:10.1016/j.cej.2012.06.155.
[117] Yu J, Wang K. Study on characteristics of steel slag for CO_2 capture. Energy Fuels. 2011;25(11):5483–92. doi:10.1021/ef2004255.
[118] Zhang X, Qian C, Ma Z, Li F. Study on preparation of supplementary cementitious material using microbial CO_2 fixation of steel slag powder. Constr Build Mater. 2022;326:126864. doi:10.1016/j.conbuildmat.2022.126864.
[119] Li Y, Pei S, Pan SY, Chiang PC, Lu C, Ouyang T. Carbonation and utilization of basic oxygen furnace slag coupled with concentrated water from electrodeionization. J CO2 Util. 2018;25:46–55. doi:10.1016/j.jcou.2018.03.003.
[120] Zhang X. Research on mass production technology of auxiliary cementitious materials prepared by CO_2 fixation in steel slag [dissertation]. Nanjing, China: Southeast University; 2023. (In Chinese).
[121] Kodama S, Nishimoto T, Yamamoto N, Yogo K, Yamada K. Development of a new pH-swing CO_2 mineralization process with a recyclable reaction solution. Energy. 2008;33(5):776–84. doi:10.1016/j.energy.2008.01.005.

[122] Owais M, Järvinen M, Taskinen P, Said A. Experimental study on the extraction of calcium, magnesium, vanadium and silicon from steelmaking slags for improved mineral carbonation of CO_2. J CO2 Util. 2019;31:1–7. doi:10.1016/j.jcou.2019.02.014.
[123] Said A, Mattila HP, Järvinen M, Zevenhoven R. Production of precipitated calcium carbonate (PCC) from steelmaking slag for fixation of CO_2. Appl Energy. 2013;112:765–71. doi:10.1016/j.apenergy.2012.12.042.
[124] Said A, Mattila O, Eloneva S, Järvinen M. Enhancement of calcium dissolution from steel slag by ultrasound. Chem Eng Process Process Intensif. 2015;89:1–8. doi:10.1016/j.cep.2014.12.008.
[125] Liu G, Tang Y, Wang J. Effects of carbonation degree of semi-dry carbonated converter steel slag on the performance of blended cement mortar–Reactivity, hydration, and strength. J Build Eng. 2023;63:105529. doi:10.1016/j.jobe.2022.105529.
[126] Chen KW, Pan SY, Chen CT, Chen YH, Chiang PC. High-gravity carbonation of basic oxygen furnace slag for CO_2 fixation and utilization in blended cement. J Clean Prod. 2016;124:350–60. doi:10.1016/j.jclepro.2016.02.072.
[127] Yang P, Ma G, Liu X, Lv G, Wang B, Yang S, et al. Design and simulation of a new carbonation device with both steel slag modification and carbon sequestration functions. Int J Heat Fluid Flow. 2024;110:109628. doi:10.1016/j.ijheatfluidflow.2024.109628.
[128] Horkoss S, Lteif R, Rizk T. Influence of the clinker SO_3 on the cement characteristics. Cem Concr Res. 2011;41(8):913–9. doi:10.1016/j.cemconres.2011.04.015.
[129] Liapis I, Papayianni I. Advances in chemical and physical properties of electric arc furnace carbon steel slag by hot stage processing and mineral mixing. J Hazard Mater. 2015;283:89–97. doi:10.1016/j.jhazmat.2014.08.072.
[130] Lian F, Ma L, Chou K. Industrial research on the high-temperature modification of Basic Oxygen Furnace slag with solid waste compound. J Clean Prod. 2017;143:549–56. doi:10.1016/j.jclepro.2016.12.075.
[131] Yin SH, Gao F, Guo H, Yang X. Phase transformation during lime reconstruction of steel slag. J South China Univ Technol Nat Sci Ed. 2016;44(6):47–52. (In Chinese).
[132] Zong YB, Cang DQ, Zhen YP, Li Y, Bai H. Component modification of steel slag in air quenching process to improve grindability. Trans Nonferrous Met Soc China. 2009;19:s834–9. doi:10.1016/S1003-6326(10)60161-6.
[133] Kitamura S, Maruoka N. Modification of stainless steel slag by mixing the nonferrous slag. In: Proceedings of the First International Slag Valorisation Symposium. Leuven, Belgium: Katholieke Universiteit Leuven; 2009. p. 93–100.
[134] He T, Li Z, Zhao S, Zhao Z, Zhao X. Effect of reductive component-conditioning materials on the composition, structure, and properties of reconstructed BOF slag. Constr Build Mater. 2020;255:119269. doi:10.1016/j.conbuildmat.2020.119269.
[135] Wang X, Ni W, Li J, Zhang S, Hitch M, Pascual R. Carbonation of steel slag and gypsum for building materials and associated reaction mechanisms. Cem Concr Res. 2019;125:105893. doi:10.1016/j.cemconres.2019.105893.
[136] Hao J, Lin Z, Wang Q, Fang K, Zhou Y, Zhuang S. Utilization of tunnel waste slurry and steel slag for preparation of backfill grouting materials: properties and hydration behavior. Clean Mater. 2025;18:100341. doi:10.1016/j.clema.2025.100341.
[137] Zhao J, Li Z, Wang D, Yan P, Luo L, Zhang H, et al. Hydration superposition effect and mechanism of steel slag powder and granulated blast furnace slag powder. Constr Build Mater. 2023;366:130101. doi:10.1016/j.conbuildmat.2022.130101.
[138] Zhuang S, Wang Q, Luo T. Modification of ultrafine blast furnace slag with steel slag as a novel high-quality mineral admixture to prepare high-strength concrete. J Build Eng. 2023;71:106501. doi:10.1016/j.jobe.2023.106501.
[139] Wang D, Na Q, Liu Y, Feng Y, Zhang Q, Chen Q. Hydration process and fluoride solidification mechanism of multi-source solid waste-based phosphogypsum cemented paste backfill under CaO modification. Cem Concr Compos. 2024;154:105804. doi:10.1016/j.cemconcomp.2024.105804.
[140] Zhuang S, Wang Q, Luo T. A quantitative method to assess and predict the exothermic behavior of steel slag blended cement. Cem Concr Res. 2024;175:107373. doi:10.1016/j.cemconres.2023.107373.
[141] Mim NJ, Shaikh FUA, Sarker PK. Sustainable 3D printed concrete incorporating alternative fine aggregates: a review. Case Stud Constr Mater. 2025;22:e04570. doi:10.1016/j.cscm.2025.e04570.
[142] Adediran A, Rajczakowska M, Steelandt A, Novakova I, Cwirzen A, Perumal P. Conventional and potential alternative non-conventional raw materials available in Nordic countries for low-carbon concrete: a review. J Build Eng. 2025;104:112384. doi:10.1016/j.jobe.2025.112384.
[143] Zong Y, Wan Q, Cang D. Preparation of anorthite-based porous ceramics using high-alumina fly ash microbeads and steel slag. Ceram Int. 2019;45(17):22445–51. doi:10.1016/j.ceramint.2019.08.003.
[144] Qian C, Hu Y, Fan Y, Rui Y. Synergistic effects and mechanisms of composite supplementary cementitious materials with carbon-fixing steel slag powder and aluminum-containing mineral admixtures. Constr Build Mater. 2024;441:137507. doi:10.1016/j.conbuildmat.2024.137507.
[145] Yang G, Li C, Xie W, Yue Y, Kong C, Li X. Effect of carbide slag and steel slag as alkali activators on the key properties of carbide slag-steel slag-slag-phosphogypsum composite cementitious materials. Front Mater. 2024;11:1353004. doi:10.3389/fmats.2024.1353004.
[146] Gu X, Wang H, Zhu Z, Liu J, Xu X, Wang Q. Synergistic effect and mechanism of lithium slag on mechanical properties and microstructure of steel slag-cement system. Constr Build Mater. 2023;396:131768. doi:10.1016/j.conbuildmat.2023.131768.
[147] Sun R, Wang D. The property, structure, and phase evolution of a binary cementitious material derived from sintering flue gas desulphurization ash and steel slag. J Build Eng. 2024;86:108908. doi:10.1016/j.jobe.2024.108908.
[148] Wu Z, Feng Z, Pu S, Zeng C, Zhao Y, Chen C, et al. Mechanical properties and environmental characteristics of the synergistic preparation of cementitious materials using electrolytic manganese residue, steel slag, and blast furnace slag. Constr Build Mater. 2024;411:134480. doi:10.1016/j.conbuildmat.2023.134480.
[149] Gu X, Wang H, Liu J, Zhu Z, Wang S, Xu X. Synergistic effects of steel slag and metakaolin in cementitious systems: packing properties, strength, and microstructure. Constr Build Mater. 2024;411:134395. doi:10.1016/j.conbuildmat.2023.134395.
[150] Huang X, Wang Z, Liu Y, Hu W, Ni W. On the use of blast furnace slag and steel slag in the preparation of green artificial reef concrete. Constr Build Mater. 2016;112:241–6. doi:10.1016/j.conbuildmat.2016.02.088.
[151] Çelik Aİ, Karalar M, Aksoylu C, Mydin MAO, Althaqafi E, Yılmaz F, et al. Effect of GBFS ratio and recycled steel tire wire on the mechanical and microstructural properties of geopolymer concrete under ambient and oven curing conditions. Case Stud Constr Mater. 2024;21:e03890. doi:10.1016/j.cscm.2024.e03890.
[152] Shan Y, Wang X, Zhuang S. Early hydration of hot-stuffy steel slag-cement composite pastes: isothermal calorimetry and phase evolution. J Sustain Cem Based Mater. 2024;13(9):1319–29. doi:10.1080/21650373.2024.2377278.
[153] Luo T, Wang X, Zhuang S. Value-added utilization of steel slag as a hydration heat controlling material to prepare sustainable and green mass concrete. Case Stud Constr Mater. 2023;19:e02619. doi:10.1016/j.cscm.2023.e02619.
[154] Wang Q, Li M, Shi M. Hydration properties of cement-steel slag-slag composite cementitious materials. J Chin Ceram Soc. 2014;42(5):629–34. (In Chinese)
[155] Xu D, Ni W, Wang Q, Xu C, Li K. Ammonia-soda residue and metallurgical slags from iron and steel industries as cementitious materials for clinker-free concretes. J Clean Prod. 2021;307:127262. doi:10.1016/j.jclepro.2021.127262.
[156] Xu C, Ni W, Li K. Effect of ammonia-soda residue on the strength and chloride-resistance performance of steel slag-granulated blast furnace slag-based concrete after immersion in artificial seawater. Materials. 2021;14(20):6048. doi:10.3390/ma14206048.
[157] Zhang M, Li K, Ni W, Zhang S, Liu Z, Wang K, et al. Preparation of mine backfilling from steel slag-based non-clinker combined with ultra-fine tailing. Constr Build Mater. 2022;320:126248. doi:10.1016/j.conbuildmat.2021.126248.
[158] Hao J, Zhou Z, Chen Z, Shen Y, Fang K, Tang F, et al. Synergistic mechanisms of steel slag, granulated blast furnace slag, and desulfurization gypsum in high-content steel slag-based cementitious backfill materials. Int J Min Sci Technol. 2025;35(6):1005–18. doi:10.1016/j.ijmst.2025.05.007.
[159] Xiang XD, Xi JC, Li CH, Jiang XW. Preparation and application of the cement-free steel slag cementitious material. Constr Build Mater. 2016;114:874–9. doi:10.1016/j.conbuildmat.2016.03.186.
[160] Hao J, Zhou Z, Chen Z, Jia R, Zhuang S, Fang K, et al. Utilization of high-volume steel slag in sustainable low carbon cementitious composites for mine backfill: synergistic mechanisms and environmental benefits. Process Saf Environ Prot. 2025;202:107689. doi:10.1016/j.psep.2025.107689.
[161] Li J, Yilmaz E, Cao S. Influence of industrial solid waste as filling material on mechanical and microstructural characteristics of cementitious backfills. Constr Build Mater. 2021;299:124288. doi:10.1016/j.conbuildmat.2021.124288.
[162] Cuesta A, Ayuela A, Aranda MAG. Belite cements and their activation. Cem Concr Res. 2021;140:106319. doi:10.1016/j.cemconres.2020.106319.
[163] Li G, Zhou C, Ahmad W, Usanova KI, Karelina M, Mohamed AM, et al. Fly ash application as supplementary cementitious material: a review. Materials. 2022;15(7):2664. doi:10.3390/ma15072664.
[164] Wang Y, Wen Z, Yang X, Gao Q. Study on development and ratio optimization of cementing material of fly ash-slag based consolidated powder. Min Res Dev. 2019;39(4):88–94. (In Chinese).
[165] Zhou M, Cheng X, Chen X. Studies on the volumetric stability and mechanical properties of cement-fly-ash-stabilized steel slag. Materials. 2021;14(3):495. doi:10.3390/ma14030495.
[166] Feng C, Li D. Reaction degree of fly ash in the cement paste. Bull Chin Ceram Soc. 2015;34(11):3202–8. (In Chinese).
[167] Geng F, Yin W, Xi Y, Shao C, Xie J, Liu S. Experimental study on pore structure of foam concrete. Bull Chin Ceram Soc. 2017;36(2):526–32. (In Chinese).
[168] Zhang Y, Zhang S, Nie Q, Shen L, Wang W. Mechanical properties and microscopic mechanism of a multi-cementitious system comprising cement, fly ash, and steel slag powder. Materials. 2023;16(22):7195. doi:10.3390/ma16227195.
[169] Song W, Zhu Z, Peng Y, Wan Y, Xu X, Pu S, et al. Effect of steel slag on fresh, hardened and microstructural properties of high-calcium fly ash based geopolymers at standard curing condition. Constr Build Mater. 2019;229:116933. doi:10.1016/j.conbuildmat.2019.116933.
[170] Guo X, Yang J. Intrinsic properties and micro-crack characteristics of ultra-high toughness fly ash/steel slag based geopolymer. Constr Build Mater. 2020;230:116965. doi:10.1016/j.conbuildmat.2019.116965.
[171] Guo X, Pan X. Effects of steel slag on mechanical properties and mechanism of fly ash–based geopolymer. J Mater Civ Eng. 2020;32(2):04019348. doi:10.1061/(asce)mt.1943-5533.0003012.
[172] Wang Q, Yan P, Mi G. Effect of blended steel slag–GBFS mineral admixture on hydration and strength of cement. Constr Build Mater. 2012;35:8–14. doi:10.1016/j.conbuildmat.2012.02.085.
[173] Pandiyan TK, Solaiyan E. Sustainable valorization of jarosite as a concrete material investigation of hydration, mechanical, and durability properties. J Sustain Metall. 2024;10(4):2352–75. doi:10.1007/s40831-024-00936-w.
[174] Zhang J, Sun N, Huo Z, Chen J. Understanding the synergistic geopolymerization mechanism of multiple solid wastes in ternary geopolymers. J Build Eng. 2024;95:110295. doi:10.1016/j.jobe.2024.110295.
[175] Sun R, Wang D, Wang Y, Fang Z, Zhang S. The effects of four typical activators on the early hydration of sintering flue gas desulphurisation ash-steel slag-cement composite cementitious material. Cem Concr Compos. 2022;131:104588. doi:10.1016/j.cemconcomp.2022.104588.
[176] Yang X, Wu S, Xu S, Chen B, Chen D, Wang F, et al. Effects of GBFS content and curing methods on the working performance and microstructure of ternary geopolymers based on high-content steel slag. Constr Build Mater. 2024;410:134128. doi:10.1016/j.conbuildmat.2023.134128.
[177] Lin JX, Liu RA, Liu LY, Zhuo KY, Chen ZB, Guo YC. High-strength and high-toughness alkali-activated composite materials: optimizing mechanical properties through synergistic utilization of steel slag, ground granulated blast furnace slag, and fly ash. Constr Build Mater. 2024;422:135811. doi:10.1016/j.conbuildmat.2024.135811.
[178] Duan S, Liao H, Cheng F, Tao M. Effect of curing condition and carbonization enhancement on mechanical properties of fly ash-desulfurization gypsum-steel slag blocks. J CO2 Util. 2020;38:282–90. doi:10.1016/j.jcou.2020.02.004.

[179] Zhang J, Jin C, Wang B, Han J, Guo L, Tang N. Study on the micro-rheological properties of fly ash-based cement mortar. Constr Build Mater. 2024;442:137664. doi:10.1016/j.conbuildmat.2024.137664.
[180] Ma G, Yan Y, Zhang M, Sanjayan J. Effect of steel slag on 3D concrete printing of geopolymer with quaternary binders. Ceram Int. 2022;48(18):26233–47. doi:10.1016/j.ceramint.2022.05.305.
[181] Mohsen A, Kohail M, Alharbi YR, Abadel AA, Soliman AM, Ramadan M. Bio-mechanical efficacy for slag/fly ash-based geopolymer mingled with mesoporous NiO. Case Stud Constr Mater. 2023;19:e02283. doi:10.1016/j.cscm.2023.e02283.
[182] Yue C, Zhao Z, Zhao D, Zhang D, Xue L. Co-treatment of steel slag and oil shale waste in cemented paste backfill: evaluation of fresh properties, microstructure, and heavy metals immobilization. J Environ Manage. 2024;349:119406. doi:10.1016/j.jenvman.2023.119406.
[183] Xu J, Chen P. Synergistic effect of iron tailings, steel slag and red mud cementitious materials on mechanical and microstructure properties. J Build Eng. 2024;95:110131. doi:10.1016/j.jobe.2024.110131.
[184] Wang F, Du H, Zheng Z, Xu D, Wang Y, Li N, et al. The impact of fly ash on the properties of cementitious materials based on slag-steel slag-gypsum solid waste. Materials. 2024;17(19):4696. doi:10.3390/ma17194696.
[185] Li Q, Wang B, Yang L, Zhou H, Kang M, Li R, et al. Synthesis of cemented paste backfill by reutilizing multiple industrial waste residues and ultrafine tailings: strength, microstructure, and GA-GPR prediction modeling. Powder Technol. 2024;434:119337. doi:10.1016/j.powtec.2023.119337.
[186] Shi C, Wang D, Wu L, Wu Z. The hydration and microstructure of ultra high-strength concrete with cement–silica fume–slag binder. Cem Concr Compos. 2015;61:44–52. doi:10.1016/j.cemconcomp.2015.04.013.
[187] Gao M, Wang J, Sha W, Guo Y. Physico-mechanical properties and synergistic hydration mechanism of steel slag-GBFS based alkali-activated composites incorporated with silica fume. J Mater Res Technol. 2025;36:3327–41. doi:10.1016/j.jmrt.2025.04.030.
[188] Zheng W, Zhao L, Zhang H, Liu Z, Pei Y, Long H. Mechanism of synergistic enhancement of hydration reaction of slag with silica fume. Iron Steel. 2022;57(5):146–55. (In Chinese).
[189] Kansal CM, Goyal R. Analysing mechanical properties of concrete with nano silica, silica fume and steel slag. Mater Today Proc. 2021;45:4520–5. doi:10.1016/j.matpr.2020.12.1032.
[190] Liu J, Wang D. Influence of steel slag-silica fume composite mineral admixture on the properties of concrete. Powder Technol. 2017;320:230–8. doi:10.1016/j.powtec.2017.07.052.
[191] Deng Y, Wang X, Zhang Y, Zhao J, Jiang A. Preparation, mechanism, and application of silica fume–steel slag composite cementitious material based on the D-optimal mixture method. Constr Build Mater. 2023;408:133638. doi:10.1016/j.conbuildmat.2023.133638.
[192] Zhang X, Zhu S, Wang Y, Li J, Li K, Zhang C. Exploration of silica fume effect on solid waste based backfilling material: mechanical properties, hydration mechanism and economic benefits. Process Saf Environ Prot. 2025;197:107042. doi:10.1016/j.psep.2025.107042.
[193] Qin Q, Meng Q, Gan M, Ma Z, Zheng Y. Deterioration mechanism of coral reef sand concrete under scouring and abrasion environment and its performance modulation. Constr Build Mater. 2023;408:133607. doi:10.1016/j.conbuildmat.2023.133607.
[194] Dong D, Huang Y, Pei Y, Zhang X, Cui N, Zhao P, et al. Effect of spherical silica fume and fly ash on the rheological property, fluidity, setting time, compressive strength, water resistance and drying shrinkage of magnesium ammonium phosphate cement. J Build Eng. 2023;63:105484. doi:10.1016/j.jobe.2022.105484.
[195] Yan Y, Zhang M, Ma G, Sanjayan J. An eco-friendly ultra-high-performance geopolymer concrete with quaternary binders for 3D printing. J Clean Prod. 2025;487:144614. doi:10.1016/j.jclepro.2024.144614.
[196] Zheng S, Liu T, Qu B, Fang C, Li L, Feng Y, et al. Experimental investigation on the effect of nano silica fume on physical properties and microstructural characteristics of lightweight cement slurry. Constr Build Mater. 2022;329:127172. doi:10.1016/j.conbuildmat.2022.127172.
[197] Xu W, Zhang Y, Liu B. Influence of silica fume and low curing temperature on mechanical property of cemented paste backfill. Constr Build Mater. 2020;254:119305. doi:10.1016/j.conbuildmat.2020.119305.
[198] Zhang W, Hao X, Wei C, Liu X, Zhang Z. Activation of low-activity calcium silicate in converter steelmaking slag based on synergy of multiple solid wastes in cementitious material. Constr Build Mater. 2022;351:128925. doi:10.1016/j.conbuildmat.2022.128925.
[199] Ke G, Yang L, Zhang H, Li Z. Comparison of hydration and macro–micro characteristics of steel slag-based and red mud-based solid waste cementitious materials. J Mater Cycles Waste Manag. 2025;27(5):3876–89. doi:10.1007/s10163-025-02354-w.
[200] Liu RX, Poon CS. Utilization of red mud derived from bauxite in self-compacting concrete. J Clean Prod. 2016;112:384–91. doi:10.1016/j.jclepro.2015.09.049.
[201] Hou D, Wu D, Wang X, Gao S, Yu R, Li M, et al. Sustainable use of red mud in ultra-high performance concrete (UHPC): design and performance evaluation. Cem Concr Compos. 2021;115:103862. doi:10.1016/j.cemconcomp.2020.103862.
[202] Zhu J, Yue H, Ma L, Li Z, Bai R. The synergistic hydration mechanism and environmental safety of multiple solid wastes in red mud-based cementitious materials. Environ Sci Pollut Res Int. 2023;30(32):79241–57. doi:10.1007/s11356-023-27800-w.
[203] Kumar S, Kumar R, Bandopadhyay A. Innovative methodologies for the utilisation of wastes from metallurgical and allied industries. Resour Conserv Recycl. 2006;48(4):301–14. doi:10.1016/j.resconrec.2006.03.003.
[204] Li T, Liu B, Fan X, Chao Y, Hou K, Chen W, et al. High-value utilization of steel slag and red mud: recovery of platinum from spent aluminum-based catalyst by pyrometallurgy. J Environ Chem Eng. 2025;13(3):116748. doi:10.1016/j.jece.2025.116748.
[205] Wang Y, Liu X, Tang B, Li Y, Zhang W, Xue Y. Effect of Ca/(Si + Al) on red mud based eco-friendly revetment block: microstructure, durability and environmental performance. Constr Build Mater. 2021;304:124618. doi:10.1016/j.conbuildmat.2021.124618.
[206] Guo X, Pan X. Mechanical properties and mechanisms of fiber reinforced fly ash–steel slag based geopolymer mortar. Constr Build Mater. 2018;179:633–41. doi:10.1016/j.conbuildmat.2018.05.198.
[207] Zhang W, Hao X, Wei C, Zeng Q, Ma S, Liu X, et al. Synergistic enhancement of converter steelmaking slag, blast furnace slag, Bayer red mud in cementitious materials: strength, phase composition, and microstructure. J Build Eng. 2022;60:105177. doi:10.1016/j.jobe.2022.105177.
[208] Li Z, Zhang J, Li S, Gao Y, Liu C, Qi Y. Effect of different gypsums on the workability and mechanical properties of red mud-slag based grouting materials. J Clean Prod. 2020;245:118759. doi:10.1016/j.jclepro.2019.118759.
[209] Hao X, Liu X, Zhang Z, Zhang W, Lu Y, Wang Y, et al. In-depth insight into the cementitious synergistic effect of steel slag and red mud on the properties of composite cementitious materials. J Build Eng. 2022;52:104449. doi:10.1016/j.jobe.2022.104449.
[210] Liu C, Wu H, Jiang J, Wang L, Kong D, Yu K. Properties of flue gas desulphurization gypsum–activated steel slag fine aggregate red mud–based concrete. J Mater Civ Eng. 2023;35(4):04023025. doi:10.1061/(asce)mt.1943-5533.0004595.
[211] Zhang J, Li S, Li Z. Investigation the synergistic effects in quaternary binder containing red mud, blast furnace slag, steel slag and flue gas desulfurization gypsum based on artificial neural networks. J Clean Prod. 2020;273:122972. doi:10.1016/j.jclepro.2020.122972.
[212] Qin H, Cao S, Yilmaz E. Mechanical, energy evolution, damage and microstructural behavior of cemented tailings-rock fill considering rock content and size effects. Constr Build Mater. 2024;411:134449. doi:10.1016/j.conbuildmat.2023.134449.
[213] Zhang B, Li K, Cai R, Liu H, Hu Y, Han B. Properties of modified superfine tailings cemented paste backfill: effects of mixing time and Al_2O_3 dosage. Constr Build Mater. 2024;417:135365. doi:10.1016/j.conbuildmat.2024.135365.
[214] Hu Y, Li K, Zhang B, Han B. Strength investigation of the cemented paste backfill in alpine regions using lab experiments and machine learning. Constr Build Mater. 2022;323(1):126583. doi:10.1016/j.conbuildmat.2022.126583.
[215] Cai M. Rockburst risk control and mitigation in deep mining. Deep Resour Eng. 2024;1(2):100019. doi:10.1016/j.deepre.2024.100019.
[216] Li M, Zhang XP, Mao SJ, Liu QS. Study of deep mining safety control decision making system. Procedia Earth Planet Sci. 2009;1(1):377–83. doi:10.1016/j.proeps.2009.09.060.
[217] Hao J, Zhou Z, Chen Z, Zhou Y, Wang J. Damage characterization and microscopic mechanism of steel slag-cemented paste backfill under uniaxial compression. Constr Build Mater. 2023;409:134175. doi:10.1016/j.conbuildmat.2023.134175.
[218] Meng G, Li M, Wu Z, Ma H, Wang Y. The effects of high temperature on the compaction behaviour of waste rock backfill materials in deep coal mines. Bull Eng Geol Environ. 2020;79(2):845–55. doi:10.1007/s10064-019-01603-1.
[219] Zhang C, Guo J, Song W, Tan Y, Taheri A, Wang X. Stability analysis and strength optimization of cemented tailings backfill in high-temperature mining. Green Smart Min Eng. 2025;2(1):84–96. doi:10.1016/j.gsme.2025.02.002.
[220] Tang B, Fan M, Yang Z, Sun Y, Yuan L. A comparison study of aggregate carbonation and concrete carbonation for the enhancement of recycled aggregate pervious concrete. Constr Build Mater. 2023;371:130797. doi:10.1016/j.conbuildmat.2023.130797.
[221] Liu L, Liu Y, Tian X, Chen X. Superior CO_2 uptake and enhanced compressive strength for carbonation curing of cement-based materials via flue gas. Constr Build Mater. 2022;346:128364. doi:10.1016/j.conbuildmat.2022.128364.
[222] Gao YH, Liu L, Fang ZY, He W, Zhang B, Zhu MB, et al. A backfill material without cementitious material: carbonation curing magnesium slag based full solid waste backfill material. J Cent South Univ. 2024;31(5):1507–25. (In Chinese). doi:10.1007/s11771-024-5635-2.
[223] Yu C, Cui C, Wang Y, Zhao J, Wu Y. Strength performance and microstructural evolution of carbonated steel slag stabilized soils in the laboratory scale. Eng Geol. 2021;295:106410. doi:10.1016/j.enggeo.2021.106410.
[224] Tian Y, Xia R, Ying Y, Lu S. Desulfurization steel slag improves the saline-sodic soil quality by replacing sodium ions and affecting soil pore structure. J Environ Manage. 2023;345:118874. doi:10.1016/j.jenvman.2023.118874.
[225] Gu X, Yu B, Dong Q, Deng Y. Application of secondary steel slag in subgrade: performance evaluation and enhancement. J Clean Prod. 2018;181(1):102–8. doi:10.1016/j.jclepro.2018.01.172.
[226] Goodarzi AR, Salimi M. Stabilization treatment of a dispersive clayey soil using granulated blast furnace slag and basic oxygen furnace slag. Appl Clay Sci. 2015;108:61–9. doi:10.1016/j.clay.2015.02.024.
[227] Manso JM, Ortega-López V, Polanco JA, Setién J. The use of ladle furnace slag in soil stabilization. Constr Build Mater. 2013;40:126–34. doi:10.1016/j.conbuildmat.2012.09.079.
[228] Liu Y, Bu Z, Cai D, Fan H, Zhang Z, Ru H, et al. Disintegration characteristics and mechanism of dispersive soil modified by Si/Ca compound system. Rock Soil Mech. 2023;44(5):1341–52. (In Chinese).
[229] Hao Z, Yang X, Xu X, Yang G. Study on repairing mechanism of wind quenching slag powder in heavy metal contaminated soil by XRD and SEM. Spectrosc Spectr Anal. 2021;41(1):278–84. (In Chinese). doi:10.3964/j.issn.1000-0593(2021)01-0278-07.
[230] Choi J, Shin WS. Application of aqueous carbonated slags in the immobilization of heavy metals in field-contaminated soils. Environ Eng Res. 2020;25(3):356–65. doi:10.4491/eer.2019.101.
[231] Yang L, Wei T, Li S, Lv Y, Miki T, Yang L, et al. Immobilization persistence of Cu, Cr, Pb, Zn ions by the addition of steel slag in acidic contaminated mine soil. J Hazard Mater. 2021;412:125176. doi:10.1016/j.jhazmat.2021.125176.
[232] Wang A, Liu Y, Zhang Y, Ren J, Zeng Y, Huang Z. Synthesis of biochar modified steel slag composites for passivation of multiple heavy metals in soil. J Environ Chem Eng. 2024;12(5):114026. doi:10.1016/j.jece.2024.114026.
[233] Jiang Q, He Y, Wu Y, Dian B, Zhang J, Li T, et al. Solidification/stabilization of soil heavy metals by alkaline industrial wastes: a critical review. Environ Pollut. 2022;312:120094. doi:10.1016/j.envpol.2022.120094.
[234] O'Connor J, Nguyen TBT, Honeyands T, Monaghan B, O'Dea D, Rinklebe J, et al. Production, characterisation, utilisation, and beneficial soil application of steel slag: a review. J Hazard Mater. 2021;419:126478. doi:10.1016/j.jhazmat.2021.126478.